

Discrete Nonholonomic LL Systems on Lie Groups

Yuri N. Fedorov

Department de Matemàtica I
Universitat Politècnica de Catalunya
Barcelona, E-08028 Spain
e-mail: yuri.fedorov@upc.es

Dmitry V. Zenkov

Department of Mathematics
North Carolina State university
Raleigh, NC 27695
e-mail: dvzenkov@unity.ncsu.edu

AMS Subject Classification 37J60, 37J35, 70H45

This version: June 21, 2005

Abstract

This paper studies discrete nonholonomic mechanical systems whose configuration space is a Lie group G . Assuming that the discrete Lagrangian and constraints are left-invariant, the discrete Euler–Lagrange equations are reduced to the discrete Euler–Poincaré–Suslov equations. The dynamics associated with the discrete Euler–Poincaré–Suslov equations is shown to evolve on a subvariety of the Lie group G . The theory is illustrated with the discrete versions of two classical nonholonomic systems, the Suslov top and the Chaplygin sleigh. The preservation of the reduced energy by the discrete flow is observed and the discrete momentum conservation is discussed.

1 Introduction

The theory of variational integrators for Lagrangian and Hamiltonian systems originated in [23], [24], and [19]. It was further developed by a number of authors (see [4], [15], [16], [25], and [18] for a more complete list of references and history). A very important feature of variational integrators is discrete momentum preservation: *If the original continuous-time system has symmetry and conserves the momentum map, so does the associated discrete-time mechanical system.*

In [6] and [14] the theory was extended to Lagrangian systems with nonholonomic constraints. In particular, it was shown in [6] that a discrete-time nonholonomic system conserves *spatial* momentum in the case of *horizontal symmetry* (see [3] for the definition of horizontal symmetry). However, the case of horizontal symmetry is not typical in nonholonomic mechanics. Apparently, Chaplygin [5] was the first to observe the link between symmetry and conservation of the components of the momentum along a *moving* frame; see also [29] and references therein. Therefore, it is natural to ask if the discrete momentum is preserved by the discrete-time nonholonomic system associated with a momentum-preserving continuous-time system in the case of nonhorizontal symmetry. A closely related question is whether the discrete dynamics has an invariant measure. We point out that continuous-time nonholonomic systems generically are not measure-preserving (see [12] and [28] for details).

This paper studies both the local and global properties of the numerical variational integrators for a nonholonomic mechanical system whose configuration space is a Lie group G . Here we consider *LL systems*, that is, we assume that both the Lagrangian and the constraint distribution are invariant with respect to the induced left action of the Lie group G on TG and $G \times G$, the phase spaces of continuous-time and discrete-time systems, respectively.

The paper is organized as follows: Section 2 gives a brief overview of both continuous and discrete-time nonholonomic dynamics. In particular, the discrete Lagrange–d’Alembert principle is reviewed.

In Section 3, nonholonomic LL systems on a Lie group G are described. The invariance of the discrete Lagrangian and constraints with respect to the left diagonal action of G on $G \times G$ enables one to introduce the *discrete Euler–Poincaré–Suslov equations* that govern the discrete momentum dynamics. Unlike the continuous-time case, the discrete momentum is shown to evolve on a *nonlinear* subvariety of the dual Lie algebra \mathfrak{g}^* of the Lie group G .¹

In Sections 4 and 5 the dynamics of the classical nonholonomic LL systems on the Lie groups $SO(3)$ and $SE(2)$ —the Suslov problem and the Chaplygin sleigh—are reviewed. The multidimensional generalizations of these problems are also treated.

In Sections 6 and 7, the discrete Suslov problem and the discrete Chaplygin sleigh are introduced and studied. The discrete flows are shown to be iterations of multi-valued maps on certain two-dimensional non-orientable subvarieties of the Lie groups $SO(3)$ and $SE(2)$. Each of these discrete models retains the existence of heteroclinic trajectories that connect the two one-parameter families of relative equilibria, which is a distinct feature of the continuous-time dynamics. If, for special values of parameters, the continuous-time system is momentum/measure preserving, then so is its discrete analogue.

Moreover, in both of the discrete models the corresponding *reduced constrained energy* is preserved as well. This property is quite unexpected; indeed, generically the discrete variational integrators, including the nonholonomic ones, do not preserve the energy.

Many other interesting problems, such as the dynamics of the discrete systems with left-invariant Lagrangian and right-invariant constraints and the discrete momentum preservation in the general case when the configuration space is not a Lie group, stayed outside the scope of this paper. These problems will be addressed in future publications.

2 Lagrangian Mechanics with Nonholonomic Constraints

In this section we briefly discuss the main concepts of continuous and discrete nonholonomic dynamics. For a complete exposition of the continuous-time model see, e.g., [1], [2], and [3].

The Euler–Lagrange Equations for Nonholonomic Systems. A nonholonomic Lagrangian system is a triple (Q, L, \mathcal{D}) , where Q is a smooth n -dimensional manifold called the *configuration space*, $L : TQ \rightarrow \mathbb{R}$ is a smooth function called the *Lagrangian*, and $\mathcal{D} \subset TQ$ is a *constraint distribution*. Recall that a distribution \mathcal{D} is a collection of linear subspaces $\mathcal{D}_q \subset T_qQ$, one for each $q \in Q$. Let $q = (q^1, \dots, q^n)$ be local coordinates on Q . In the induced coordinates (q, \dot{q}) on the tangent bundle TQ we write $L(q, \dot{q})$. It is assumed that the Lagrangian is *hyperregular*, *i.e.*, the map

$$\frac{\partial L}{\partial \dot{q}} : TQ \rightarrow T^*Q$$

is invertible (see [17]).

A curve $q(t) \in Q$ is said to *satisfy the constraints* if $\dot{q}(t) \in \mathcal{D}_{q(t)}$ for all t . The dynamics of the system is given by the following *Lagrange–d’Alembert principle*: *The equations of motion for the system are those determined by*

$$\delta \int_a^b L(q^i, \dot{q}^i) dt = 0, \tag{2.1}$$

where we choose variations $\delta q(t)$ of the curve $q(t)$ that satisfy $\delta q(a) = \delta q(b) = 0$ and $\delta \dot{q}(t) \in \mathcal{D}_{q(t)}$ for each $t \in [a, b]$. This principle is supplemented by the condition that the curve itself satisfies the constraints. Note that we take the variation *before* imposing the constraints; that is, we do not impose the constraints on the family of curves defining the variation. This is well known to be important to obtain the correct mechanical equations (see, e.g., [1] and [3] for a discussion and references).

¹In the continuous-time case, the momentum is restricted to a linear subspace of \mathfrak{g}^* .

Assuming that the constraint distribution is specified by a set of s differential forms $A^j(q)$, $j = 1, \dots, s$, that is,

$$\mathcal{D} = \{\dot{q} \in TQ \mid \langle A^j(q), \dot{q} \rangle = 0, j = 1, \dots, s\}, \quad (2.2)$$

equation (2.1) implies

$$\frac{d}{dt} \frac{\partial L}{\partial \dot{q}} - \frac{\partial L}{\partial q} = \sum_{j=1}^s \lambda_j A^j(q). \quad (2.3)$$

Equations (2.3) are called the *Euler–Lagrange equations with multipliers*. Coupled with (2.2), they give a complete description of the dynamics of the system.

Theorem 2.1. *Equations (2.3) conserve the energy*

$$E = \left\langle \frac{\partial L}{\partial \dot{q}}, \dot{q} \right\rangle - L. \quad (2.4)$$

See [2] for the proof and discussion.

The Euler–Poincaré–Suslov Equations. Now let the configuration space be an n -dimensional connected Lie group G with local coordinates g . As usual, we use the notation $[\cdot, \cdot] : \mathfrak{g} \times \mathfrak{g} \rightarrow \mathfrak{g}$ for the antisymmetric bracket operation on the Lie algebra $\mathfrak{g} = T_e G$ of the group G . Define an *LL system* on G as a Lagrangian system (G, L, \mathcal{D}) with a left-invariant Lagrangian $L : TG \rightarrow \mathbb{R}$ and a left-invariant (generally nonintegrable) distribution \mathcal{D} on the tangent bundle TG .

The Lagrangian $L : TG \rightarrow \mathbb{R}$ is left-invariant if and only if $L(g, \dot{g})$ depends on (g, \dot{g}) through the *body velocity operator* $\omega = g^{-1} \dot{g} = TL_{g^{-1}} \dot{g}$. Then there exists a function $l : \mathfrak{g} \rightarrow \mathbb{R}$ called the *reduced Lagrangian* such that $L(g, \dot{g}) = l(\omega)$.

A distribution $\mathcal{D} \subset TG$ is left-invariant if and only if there is a subspace $\mathfrak{d} \subset \mathfrak{g}$ such that $\mathcal{D}_g = TL_g \mathfrak{d} \subset T_g G$ for any $g \in G$. Let \mathfrak{g}^* be the dual of the Lie algebra \mathfrak{g} and let $a^j \in \mathfrak{g}^*$, $j = 1, \dots, s$, be independent annihilators of the subspace \mathfrak{d} , *i.e.*,

$$\mathfrak{d} = \{\xi \in \mathfrak{g} \mid \langle a^j, \xi \rangle = 0, j = 1, \dots, s\}, \quad (2.5)$$

where $\langle \cdot, \cdot \rangle : \mathfrak{g}^* \times \mathfrak{g} \rightarrow \mathbb{R}$ is the standard pairing. The left-invariant constraints on TG are defined by the equations

$$\langle a^j, g^{-1} \dot{g} \rangle = 0, \quad j = 1, \dots, s.$$

Define the *body momentum* $p : \mathfrak{g} \rightarrow \mathfrak{g}^*$ by the formula $p = \partial l / \partial \omega$. According to [13], the *reduced dynamics* of an LL system (G, L, \mathcal{D}) is governed by the *Euler–Poincaré–Suslov equations with multipliers*

$$\dot{p} = \text{ad}_\omega^* p + \sum_{j=1}^s \lambda_j a^j \quad (2.6)$$

coupled with the constraints (2.5). The dynamics of the group variables g is obtained by solving the *reconstruction equation*

$$\dot{g} = TL_g \omega. \quad (2.7)$$

Remark. In the absence of constraints, equations (2.6) become the Euler–Poincaré equations, which conserve the *spatial momentum* $J = \text{Ad}_g^* p$. In the presence of nonholonomic constraints, neither the spatial nor body momentum is conserved generically. The conditions for body momentum preservation are studied in [29].

Theorem 2.2. *The Euler–Poincaré–Suslov equations conserve the **reduced constrained energy***

$$E_c = [\langle p, \omega \rangle - l(\omega)]_{\omega \in \mathfrak{d}}.$$

Proof. Observe that the reduced energy $\langle p, \omega \rangle - l(\omega)$ equals the energy, as the Lagrangian is left-invariant. Since $\omega \in \mathfrak{d}$ throughout the motion, the reduced constrained energy equals the energy along the trajectories of (2.6) and therefore is preserved.² \square

Let the reduced Lagrangian $l(\omega)$ be the quadratic form $l = \frac{1}{2}\langle \mathbb{I}\omega, \omega \rangle$, where $\mathbb{I} : \mathfrak{g} \rightarrow \mathfrak{g}^*$ is a symmetric non-singular *inertia operator*. In this case, $p = \mathbb{I}\omega$. Then constraints (2.5) imply that p lies in the subspace

$$\mathfrak{d}^* = \{\langle a^j, \mathbb{I}^{-1}p \rangle = 0, j = 1, \dots, s\} \subset \mathfrak{g}^*.$$

It is often convenient to choose a basis e_1, \dots, e_n in the Lie algebra \mathfrak{g} such that $a^j = e^{n-j+1}$, $j = 1, \dots, s$. Let ω_i, p_i , and \mathbb{I}_{ij} denote the components of ω, p , and \mathbb{I} relative to this basis, respectively. Then the formula representing the reduced constrained energy becomes

$$\frac{1}{2} \sum_{i,j=1}^{n-s} \mathbb{I}_{ij} \omega_i \omega_j = \frac{1}{2} \sum_{i,j=1}^{n-s} I^{ij} p_i p_j. \quad (2.8)$$

Here and elsewhere, the quantities I^{ij} represent the components of the *inverse constrained inertia operator* $(\mathbb{I}|_{\mathfrak{d}})^{-1}$.

Discrete Mechanical Systems with Nonholonomic Constraints. According to [6], a discrete nonholonomic mechanical system on a smooth n -dimensional manifold Q is specified by

- (i) a *discrete Lagrangian* $L_d : Q \times Q \rightarrow \mathbb{R}$;
- (ii) an $(n - s)$ -dimensional distribution \mathcal{D} on TQ given by equations (2.2);
- (iii) a discrete constraint manifold $\mathcal{D}_d \subset Q \times Q$, which has the same dimension as \mathcal{D} and satisfies the condition $(q, q) \in \mathcal{D}_d$ for all $q \in Q$.

The dynamics is given by the following *discrete Lagrange-d'Alembert principle* (see [6]):

$$\sum_{k=0}^{N-1} \left(D_1 L_d(q_k, q_{k+1}) + D_2 L_d(q_{k-1}, q_k) \right) \delta q_k = 0, \quad \delta q_k \in \mathcal{D}_{q_k}, \quad (q_k, q_{k+1}) \in \mathcal{D}_d.$$

Here $D_1 L_d$ and $D_2 L_d$ denote the partial derivatives of the discrete Lagrangian with respect to the first and the second inputs, respectively.

The discrete constraint manifold is usually specified by the *discrete constraint functions*

$$\mathcal{F}_j(q_k, q_{k+1}) = 0, \quad j = 1, \dots, s. \quad (2.9)$$

The dynamics of a discrete nonholonomic system is represented by sequences $\{(q_k, q_{k+1})\}$ that satisfy the *discrete Lagrange-d'Alembert equations with multipliers*

$$D_1 L_d(q_k, q_{k+1}) + D_2 L_d(q_{k-1}, q_k) = \sum_{j=1}^s \lambda_k^j A^j(q_k), \quad (2.10)$$

where $A^j(q)$ are the constraint one-forms from (2.2).

According to [6], the map $(q_{k-1}, q_k) \mapsto (q_k, q_{k+1})$ defined by equations (2.9) and (2.10) is a local diffeomorphism in a neighborhood of the diagonal of $Q \times Q$ if the matrix

$$\begin{pmatrix} D_1 D_2 L_d(q, q') & A^1(q) & \cdots & A^s(q) \\ D_2 \mathcal{F}_1(q, q') & 0 & \cdots & 0 \\ \vdots & \vdots & \ddots & \vdots \\ D_2 \mathcal{F}_s(q, q') & 0 & \cdots & 0 \end{pmatrix}$$

²We will see later that the discrete analogues of the reduced energy and the reduced constrained energy have *different* conservation properties.

is invertible for each (q, q') from this neighborhood.

One way to construct the discrete Lagrangian is to set $L_d = L \circ \Psi$, where $\Psi : Q \times Q \rightarrow TQ$ is the *discretization map*. In this case the discrete constraint manifold \mathcal{D}_d has to be consistent with the distribution \mathcal{D} , that is, \mathcal{D}_d has to be locally defined as $A^j \circ \Psi = 0$, $j = 1, \dots, s$. If the configuration space is \mathbb{R}^n , it is natural to choose

$$\Psi(q_k, q_{k+1}) = \left(\frac{q_{k+1} + q_k}{2}, \frac{q_{k+1} - q_k}{h} \right) \in T\mathbb{R}^n, \quad (2.11)$$

where $h \in \mathbb{R}_+$ is the *time step* (see [16] and [6] for details). We emphasize that the discretization map is not unique and hence there are many ways to define the discrete Lagrangian L_d and the discrete constraint manifold \mathcal{D}_d for a given nonholonomic system (Q, L, \mathcal{D}) .³

3 Discrete Euler–Poincaré–Suslov Equations

In this section we obtain the reduced equations of motion of discrete nonholonomic systems on Lie groups.

Continuous and Discrete Left-Invariant Lagrangians. Let the configuration space be a Lie group G with local coordinates g . Let the discrete Lagrangian $L_d : G \times G \rightarrow \mathbb{R}$ be invariant with respect to the left diagonal action of G on $G \times G$, that is

$$L_d(gg_k, gg_{k+1}) = L_d(g_k, g_{k+1})$$

for any $g \in G$.

Define the *left incremental displacement* by the formula $W_k = g_k^{-1}g_{k+1} \in G$. Since L_d is left-invariant, there exists a function $l_d : (G \times G)/G \cong G \rightarrow \mathbb{R}$ called the *reduced discrete Lagrangian* such that $L_d(g_k, g_{k+1}) = l_d(W_k)$. According to [16], one defines the discrete constrained Lagrangian l_d associated with a given continuous left-invariant Lagrangian $L(g, \dot{g}) = l(g^{-1}\dot{g})$ by the formula $l_d = l((\log W_k)/h)$, where $\log : G \rightarrow \mathfrak{g}$ is the (local) inverse of the exponential map $\exp : \mathfrak{g} \rightarrow G$ and $h \in \mathbb{R}_+$ is the given time step.

For a matrix group G , one can instead use the approximation

$$(\log W_k)/h \approx (W_k - e)/h = g_k^{-1}(g_{k+1} - g_k)/h$$

and define the discrete Lagrangian by the formula

$$L_d(g_k, g_{k+1}) = l(g_k^{-1}(g_{k+1} - g_k)/h). \quad (3.1)$$

For quadratic Lagrangians considered later in this paper the value of the time step h does not influence the dynamics. We thus set $h = 1$ in the rest of the paper.

Similarly to [4] and [16], we define the *discrete body momentum* $p_k : G \times G \rightarrow \mathfrak{g}^*$ by the formula

$$\langle p_k, \xi \rangle = -\frac{d}{ds} \Big|_{s=0} L_d(g_k \exp(s\xi), g_{k+1}) = -\frac{d}{ds} \Big|_{s=0} l_d(\exp(-s\xi)W_k) \quad (3.2)$$

for any $\xi \in \mathfrak{g}$.⁴ Definition (3.2) implies

$$p_k = -L_{g_k}^* D_1 L_d(g_{k-1}, g_k) = R_{W_k}^* l'_d(W_k), \quad (3.3)$$

³An alternative approach to the discretization of nonholonomic systems based on a modification of canonical transformations was proposed in [14].

⁴The definition of the discrete momentum (3.2) accepted in this paper varies slightly from that used in many publications,

$$\langle p_k, \xi \rangle = \frac{d}{ds} \Big|_{s=0} L_d(g_{k-1}, g_k \exp(s\xi)).$$

where $L_g^* : T^*G \rightarrow \mathfrak{g}^*$ and $R_g^* : T^*G \rightarrow \mathfrak{g}^*$ are the induced left and right actions, respectively.

Using (3.2), one defines the *discrete Legendre transform*

$$\mathcal{L} : G \times G \ni (g_k, W_k) \mapsto (g_k, p_k) \in G \times \mathfrak{g}^*,$$

which is invertible in a neighborhood of the set $\{(g, p) \in G \times \mathfrak{g}^* \mid p = 0\}$, but may fail to be globally invertible.

Discrete Left-Invariant Constraints. If the continuous constraint distribution \mathcal{D} is left-invariant, it is natural to require that the discrete constraint manifold \mathcal{D}_d is invariant with respect to the left diagonal action of G on $G \times G$, that is,

$$\mathcal{F}_j(gg_k, gg_{k+1}) = \mathcal{F}_j(g_k, g_{k+1}) \quad \text{for any } g \in G, \quad j = 1, \dots, s.$$

This implies that there exist functions $f_j : G \rightarrow \mathbb{R}$, $j = 1, \dots, s$, such that

$$\mathcal{F}_j(g_k, g_{k+1}) = f_j(W_k).$$

Consequently, $\mathcal{D}_d \subset G \times G$ is completely defined by the *constrained (or admissible) displacement subvariety*

$$\mathcal{S} = \{f_1(W) = 0, \dots, f_s(W) = 0\} \subset G;$$

that is, $\mathcal{D}_d = \{(g, g') \in G \times G \mid g^{-1}g' \in \mathcal{S}\}$.

The subvariety \mathcal{S} passes through the identity element $e \in G$, and the tangent space $T_e\mathcal{S}$ coincides with the linear subspace $\mathfrak{d} \subset \mathfrak{g}$ associated with the left-invariant distribution $\mathcal{D} \subset TG$. Motivated by this, we define \mathcal{S} as the union of all one-parameter subgroups G_η generated by vectors $\eta \in \mathfrak{d}$, *i.e.*, $\mathcal{S} = \exp \mathfrak{d}$. In the vicinity of the identity element $e \in G$ one can equivalently write

$$\mathcal{S} = \{W \in G \mid \log W \in \mathfrak{d}\}. \quad (3.4)$$

Remark. For an arbitrary subspace $\mathfrak{d} \subset \mathfrak{g}$, the set $\exp \mathfrak{d}$ is not necessarily a subvariety of G . In this paper we concentrate on the important case when G contains a subgroup H generated by a subalgebra $\mathfrak{h} \subset \mathfrak{g}$ such that the decomposition $\mathfrak{g} = \mathfrak{h} \oplus \mathfrak{d}$ forms a symmetric pair, that is

$$[\mathfrak{h}, \mathfrak{h}] \subset \mathfrak{h}, \quad [\mathfrak{d}, \mathfrak{d}] \subset \mathfrak{h}, \quad [\mathfrak{h}, \mathfrak{d}] \subset \mathfrak{d}. \quad (3.5)$$

In this case the following property holds (see, e.g., [11]):

Proposition 3.1. *If \mathfrak{d} and \mathfrak{h} form a symmetric pair, then the set $\mathcal{S} = \exp \mathfrak{d}$ is a smooth submanifold of G homeomorphic to either the symmetric space G/H or to a quotient of G/H resulting from a finite group action.*

If conditions (3.5) are satisfied, the set $\exp \mathfrak{d}$ is known as the Cartan model of the symmetric space G/H . Notice also that the tangent bundle $T\mathcal{S}$ is not a subset of the left-invariant distribution $\mathcal{D} \subset TG$, since the latter is not integrable.

Using the Legendre transform \mathcal{L} , we conclude that the discrete momentum p_k is restricted to the subvariety

$$\mathcal{U} = \mathcal{L}(\mathcal{S}) = \{p \in \mathfrak{g}^* \mid p = R_W^* l'_d(W), W \in \mathcal{S}\} \subset \mathfrak{g}^*.$$

In the examples considered below, the map $\mathcal{S} \rightarrow \mathcal{U}$ is invertible almost everywhere on \mathcal{S} .

Discrete Euler–Poincaré–Suslov Equations. Assume that the discrete Lagrangian $L_d : G \times G \rightarrow \mathbb{R}$, the discrete constraint manifold $\mathcal{D}_d \subset G \times G$, and the constraint distribution $\mathcal{D} \subset TG$ are left-invariant with respect to the induced left actions of G on $G \times G$ and on TG , accordingly.

Define the *action sum* and the *reduced action sum* by the formulae

$$S_d = \sum_{k=0}^{N-1} L_d(g_k, g_{k+1}) \quad \text{and} \quad s_d = \sum_{k=0}^{N-1} l_d(W_k).$$

Recall that the distribution \mathcal{D} is written as $\langle A^j(g), \dot{g} \rangle = 0$, $j = 1, \dots, s$. According to [6], variations δg_k satisfy the conditions $\langle A^j(g_k), \delta g_k \rangle = 0$, $j = 1, \dots, s$, and $\delta g_0 = \delta g_N = 0$. For the left-invariant constraints given by (2.5), the admissible discrete variations are those $\delta g_k \in TG_{g_k}$ that satisfy the conditions

$$\langle a^j, g_k^{-1} \delta g_k \rangle = 0, \quad j = 1, \dots, s, \quad k = 1, \dots, N-1. \quad (3.6)$$

The following theorem extends the results of Bobenko and Suris [4] and Marsden, Pekarsky, and Shkoller [16] to the nonholonomic setting.

Theorem 3.2. *Let $L_d : G \times G \rightarrow \mathbb{R}$ be a left-invariant Lagrangian, $l_d : G \rightarrow \mathbb{R}$ be the reduced Lagrangian, and $\mathcal{D} \subset TQ$ and $\mathcal{D}_d \subset Q \times Q$ be the constraint distribution and discrete constraint manifold, respectively. Then the following statements are equivalent:*

- (i) *The sequence $\{(g_k, g_{k+1})\}_{k=0}^{N-1}$ is a critical point of the action sum $S_d : G^{N-1} \rightarrow \mathbb{R}$ for arbitrary constrained variations.*
- (ii) *The sequence $\{(g_k, g_{k+1})\}_{k=0}^{N-1}$ satisfies the discrete Euler–Lagrange equations with multipliers*

$$D_1 L_d(g_k, g_{k+1}) + D_2 L_d(g_{k-1}, g_k) = - \sum_{j=1}^s \lambda_k^j A^j(g_k) \quad (3.7)$$

coupled with the discrete constraint equations $\mathcal{F}_j(g_k, g_{k+1}) = 0$.

- (iii) *The sequence $\{W_k\}_{k=0}^{N-1}$ is a critical point of the reduced action sum $s_d : G^{N-1} \rightarrow \mathbb{R}$ with respect to variations δW_k , induced by the constrained variations δg_k and given by*

$$\delta W_k = W_k \left[g_{k+1}^{-1} \delta g_{k+1} - \text{Ad}_{W_k^{-1}} g_k^{-1} \delta g_k \right]. \quad (3.8)$$

- (iv) *The sequence $\{W_k\}_{k=0}^{N-1}$ satisfies the equations*

$$l'_d(W_{k-1}) T L_{W_{k-1}} - l'_d(W_k) T L_{W_k} \text{Ad}_{W_k^{-1}} = - \sum_{j=1}^s \lambda_k^j a^j \quad (3.9)$$

coupled with the discrete constraint equations

$$f_j(W_k) = 0, \quad j = 1, \dots, s, \quad k = 1, \dots, N-1.$$

Proof. We first prove the equivalence of (i) and (ii) following [6]. Recall that the variations δg_k vanish at $k = 0$ and $k = N$. Computing the first variation of the discrete action sum S_d , we obtain

$$\delta S_d = \sum_{k=1}^{N-1} (D_1 L_d(g_k, g_{k+1}) + D_2 L_d(g_{k-1}, g_k)) \delta g_k.$$

Here the variations δg_k are not independent and satisfy the conditions $\langle A^j(g_k), \delta g_k \rangle = 0$. Therefore, $\delta S_d = 0$ if and only if g_k , $k = 1, \dots, N-1$, satisfy equations (3.7).

Next, we prove that (i) is equivalent to (iii). Notice that $L_d = l_d \circ \pi$, where $\pi : G \times G \rightarrow (G \times G)/G \cong G$ is given by $(g_k, g_{k+1}) \mapsto g_k^{-1} g_{k+1}$. Therefore $\delta s_d = \delta S_d$. The variation δW_k is computed to be

$$\delta W_k = g_k^{-1} \delta g_{k+1} - g_k^{-1} \delta g_k g_k^{-1} g_{k+1} = g_k^{-1} g_{k+1} \left[g_{k+1}^{-1} \delta g_{k+1} - \text{Ad}_{(g_k^{-1} g_{k+1})^{-1}} (g_k^{-1} \delta g_k) \right],$$

which yields (3.8).

To prove the equivalence of (iii) and (iv), we use (3.8) to compute

$$\delta s_d = \sum_{k=1}^{N-1} \left[l'_d(g_{k-1}^{-1} g_k) T L_{g_{k-1}^{-1} g_k} - l'_d(g_k^{-1} g_{k+1}) T L_{g_k^{-1} g_{k+1}} \text{Ad}_{(g_k^{-1} g_{k+1})^{-1}} \right] (g_k^{-1} \delta g_k).$$

Since the variations δg_k satisfy conditions (3.6), $\delta s_d = 0$ if and only if item (iv) holds. \square

We now rewrite (3.9) in the form of discrete momentum equations.

Theorem 3.3. *The discrete momentum evolution is governed by the **discrete Euler–Poincaré–Suslov equations***

$$p_{k+1} - \text{Ad}_{W_k}^* p_k = \sum_{j=1}^s \lambda_{k+1}^j a^j, \quad (3.10)$$

where W_k is restricted to \mathcal{S} and $p_k \in \mathcal{U} \subset \mathfrak{g}^*$.

Proof. Using definition (3.3), one has $l'_d(W_k) = TR_{W_k}^* p_k$, and therefore for any $\eta \in \mathfrak{g}$,

$$l'_d(W_{k-1})TL_{W_{k-1}}\eta = \langle TR_{W_{k-1}}^* p_k, TL_{W_{k-1}}\eta \rangle = \langle TL_{W_{k-1}}^* TR_{W_{k-1}}^* p_{k-1}, \eta \rangle = \langle \text{Ad}_{W_{k-1}}^* p_{k-1}, \eta \rangle.$$

Similarly,

$$l'_d(W_k)TL_{W_k}\text{Ad}_{W_k^{-1}}\eta = \langle \text{Ad}_{W_k}^* p_k, \text{Ad}_{W_k^{-1}}\eta \rangle = \langle \text{Ad}_{W_k^{-1}}^* \text{Ad}_{W_k}^* p_k, \eta \rangle = \langle p_k, \eta \rangle.$$

Thus, (3.9) becomes (3.10), where W_k is restricted to \mathcal{S} and $p_k \in \mathcal{U} \subset \mathfrak{g}^*$. \square

Equations (3.10) generalize the discrete Euler–Poincaré equations obtained in [4] and [16] to the nonholonomic setting and define a map $\mathcal{B} : \mathcal{U} \rightarrow \mathcal{U}$ that takes p_k to p_{k+1} . The map \mathcal{B} is generally multi-valued. Given p_k , one evaluates p_{k+1} by

1. Inverting the map $p_k = R_{W_k}^* l'_d(W_k)$ and finding the associated value(s) of W_k .
2. Calculating $\text{Ad}_{W_k}^* p_k$.
3. Projecting $\text{Ad}_{W_k}^* p_k$ onto \mathcal{U} along the subspace $\text{span}(a^1, \dots, a^s)$.

Since the map \mathcal{B} is multi-valued, one needs to make a choice of a branch of \mathcal{B} . A natural way of doing this is to start from a value of p_k whose norm is small and to select p_{k+1} of the smallest norm.

4 The Suslov Problem

The first known example of an LL system, the Suslov problem, was originally introduced in 1902 in [22]. The Suslov problem studies the motion of a rigid body suspended at its center of mass in the presence of a constraint that forces the projection of the body angular velocity along a direction fixed in body to vanish.

The Classical Suslov Problem. Here we briefly review the dynamics of the Suslov problem. We refer the reader to [22] and [2] for a complete exposition.

The configuration space for this problem is the group $SO(3)$. The Lie algebra $so(3)$ is isomorphic to the Euclidean vector space \mathbb{R}^3 . The isomorphism $\varphi : so(3) \rightarrow \mathbb{R}^3$ is given by

$$\varphi(\omega) = (\omega_1, \omega_2, \omega_3) \in \mathbb{R}^3, \quad \text{where } \omega = \begin{pmatrix} 0 & -\omega_3 & \omega_2 \\ \omega_3 & 0 & -\omega_1 \\ -\omega_2 & \omega_1 & 0 \end{pmatrix} \in so(3).$$

In this representation of $so(3)$ the antisymmetric bracket operation is the standard vector product in \mathbb{R}^3 . The elements of $so(3)$, when viewed as vectors from \mathbb{R}^3 , are typed in bold.

Let $\mathbb{I} = (\mathbb{I}_{ij})$ be the inertia operator of the body, $\mathbb{I}^{-1} = (\mathbb{I}^{ij})$ be its inverse, and $\boldsymbol{\omega} \in \mathbb{R}^3$ be the body angular velocity vector. The reduced Lagrangian equals $l = \frac{1}{2} \langle \mathbb{I} \boldsymbol{\omega}, \boldsymbol{\omega} \rangle$. Let \boldsymbol{a} be the direction, fixed in the body, of the vanishing component of the angular velocity. The constraint reads

$$\langle \boldsymbol{a}, \boldsymbol{\omega} \rangle = 0. \quad (4.1)$$

The Lagrangian and constraint are left-invariant with respect to the lifted action of $SO(3)$ on $TSO(3)$.

Using the Killing metric, one identifies the dual Lie algebra $so^*(3)$ and the Lie algebra $so(3)$. Using this identification, the body angular momentum $\mathbf{M} = \partial l / \partial \boldsymbol{\omega}$ becomes an element of $so(3)$, and the Euler–Poincaré–Suslov equations (2.6) written for the Suslov problem become

$$\dot{\mathbf{M}} = \mathbf{M} \times \boldsymbol{\omega} + \lambda \mathbf{a}. \quad (4.2)$$

Eliminating the Lagrange multiplier, we obtain

$$\dot{\mathbf{M}} = \frac{1}{\langle \mathbf{a}, \mathbb{I}^{-1} \mathbf{a} \rangle} \langle \mathbf{a}, \mathbf{M} \rangle (\mathbb{I}^{-1} \mathbf{a} \times \boldsymbol{\omega}). \quad (4.3)$$

Without loss of generality, let us choose \mathbf{a} as the third vector of the body frame $\mathbf{e}_1, \mathbf{e}_2, \mathbf{e}_3$. Then the constraint becomes $\omega_3 = 0$, and the momentum is restricted to the subspace

$$\mathfrak{d}^* = \{\mathbb{I}^{31} M_1 + \mathbb{I}^{32} M_2 + \mathbb{I}^{33} M_3 = 0\}. \quad (4.4)$$

Select (M_1, M_2) as coordinates in \mathfrak{d}^* . Then the momentum dynamics is governed by the equations

$$\dot{M}_1 = (\mathbb{I}^{31} M_1 + \mathbb{I}^{32} M_2) \omega_2 / \mathbb{I}^{33}, \quad \dot{M}_2 = -(\mathbb{I}^{31} M_1 + \mathbb{I}^{32} M_2) \omega_1 / \mathbb{I}^{33}. \quad (4.5)$$

The Suslov problem preserves both the energy $E = \frac{1}{2} \langle \mathbb{I} \boldsymbol{\omega}, \boldsymbol{\omega} \rangle$ and the reduced constrained energy $E_c = E|_{\mathfrak{d}}$. If $\mathbf{a} = \mathbf{e}_3$, the reduced constrained energy becomes

$$E_c = \frac{1}{2} (\mathbb{I}_{11} \omega_1^2 + 2\mathbb{I}_{12} \omega_1 \omega_2 + \mathbb{I}_{22} \omega_2^2) = \frac{\mathbb{I}_{22} M_1^2 - 2\mathbb{I}_{12} M_1 M_2 + \mathbb{I}_{11} M_2^2}{2(\mathbb{I}_{11} \mathbb{I}_{22} - (\mathbb{I}_{12})^2)}. \quad (4.6)$$

The momentum trajectories in the $M_1 M_2$ -plane are the elliptic arcs that form the heteroclinic connections between the asymptotically stable and unstable equilibria.

The dynamics of the group variables for the Suslov problem is obtained by solving the reconstruction equation

$$\dot{g} = g\boldsymbol{\omega}.$$

The equilibria of (4.5) correspond to the steady-state rotations of the rigid body. The non-equilibrium trajectories of (4.5) generate the transitional solutions that asymptotically approach these steady-state rotations as $t \rightarrow \pm\infty$.

The Generalized Suslov Problem. Certain natural multidimensional generalizations of the Suslov problem were studied in [7], [10], and [27]. The configuration space of an n -dimensional rigid body with a fixed point is the Lie group $SO(n)$. For a path $g(t) \in SO(n)$, the angular velocity of the body is defined as $\boldsymbol{\omega}(t) = g^{-1} \dot{g}(t) \in so(n)$.

Let $\mathbb{I} : so(n) \rightarrow so^*(n)$ be a symmetric non-singular inertia operator. The reduced Lagrangian for the generalized rigid body is

$$l = \frac{1}{2} \langle \mathbb{I} \boldsymbol{\omega}, \boldsymbol{\omega} \rangle. \quad (4.7)$$

The inertia operator is often defined by the formula

$$\mathbb{I} \boldsymbol{\omega} = J\boldsymbol{\omega} + \boldsymbol{\omega} J \in so^*(n), \quad (4.8)$$

where J is a symmetric positive-definite non-singular $n \times n$ matrix called the *mass tensor* (see, e.g., [7]). Although definition (4.8) is not unique, it is widely accepted because \mathbb{I} in (4.8) for $n = 3$ represents the inertia operator for the physical three-dimensional rigid body. Utilizing formula (4.8) we obtain the formula for the body momentum: $M = J\boldsymbol{\omega} + \boldsymbol{\omega} J \in so^*(n)$.

Let e_1, \dots, e_n be an orthogonal (relative to the standard metric in \mathbb{R}^n) body frame, and let e^1, \dots, e^n be the dual basis, i.e., $\langle e^i, e_j \rangle = \delta_j^i$, where δ_j^i is the usual Kronecker delta. The generalized Suslov constraints are chosen to be

$$\langle e^i \wedge e^j, \boldsymbol{\omega} \rangle = 0, \quad 1 \leq i < j \leq n-1, \quad (4.9)$$

as in [7], *i.e.*, the angular velocity ω belongs to the subspace of matrices of the form

$$\begin{pmatrix} 0 & \dots & 0 & \omega_{1n} \\ \vdots & \ddots & \vdots & \vdots \\ 0 & \dots & 0 & \omega_{n-1,n} \\ -\omega_{1n} & \dots & -\omega_{n-1,n} & 0 \end{pmatrix}. \quad (4.10)$$

This choice is motivated by the following interpretation of the classical Suslov constraint. Assuming $\mathbf{a} = \mathbf{e}_3$, constraint (4.1) restricts the infinitesimal rotations of the three-dimensional rigid body to the planes that pass through \mathbf{e}_3 . Building on this observation, it is natural to define the n -dimensional Suslov constraints by forcing the infinitesimal rotations into the 2-dimensional subspaces of \mathbb{R}^n that contain the vector \mathbf{e}_n . The angular velocities corresponding to such infinitesimal rotations are those satisfying conditions (4.9). Hence, the dynamics of the multidimensional Suslov problem is governed by the equations with multipliers

$$\dot{M} = \text{ad}_\omega^* M + \sum_{1 \leq i < j \leq n-1} \lambda_{ij} e^i \wedge e^j \quad (4.11)$$

coupled with the constraints (4.9). For $n = 3$ the Lie algebra $so(3)$ is isomorphic to \mathbb{R}^3 and (4.11) become equations (4.2).

Let $\Lambda : \mathfrak{d} \rightarrow \mathfrak{d}^*$ be the restriction of the inertia operator \mathbb{I} onto the subspace \mathfrak{d} . The operator Λ is non-singular, and its matrix relative to the basis $\{e_1 \wedge e_n, \dots, e_{n-1} \wedge e_n\}$ is

$$\Lambda_{ij} = J_{ij} + J_{nn} \delta_{ij}, \quad i, j = 1, \dots, n-1.$$

The off-diagonal entries J_{ij} , $1 \leq i < j \leq n-1$, can be annihilated by a suitable orthogonal transformation that leaves the vector \mathbf{e}_n and the constraints (4.9) unchanged. Put $\mathcal{J} = (J_{1n}, \dots, J_{n-1,n})$ and $\varpi = (\omega_{1n}, \dots, \omega_{n-1,n})$. Using (4.11), we obtain the following closed system for the variables $\omega_{1n}, \dots, \omega_{n-1,n}$:

$$(J_{ii} + J_{nn})\dot{\omega}_{in} = J_{in}(\omega_{1n}^2 + \dots + \omega_{n-1,n}^2) - (J_{1n}\omega_{1n} + \dots + J_{n-1,n}\omega_{n-1,n})\omega_{in},$$

or, in the vector form,

$$\Lambda \dot{\varpi} = (\varpi \wedge \mathcal{J}) \varpi. \quad (4.12)$$

The equations for the remaining components ω_{ij} determine the multipliers λ_{ij} .

Equations (4.11) conserve the constrained energy

$$E = \frac{1}{2} \langle \Lambda \varpi, \varpi \rangle = \frac{1}{2} \langle \mathcal{M}, \Lambda^{-1} \mathcal{M} \rangle, \quad (4.13)$$

where $\mathcal{M} = (M_{1n}, \dots, M_{n-1,n})$. Since Λ is positive-definite, we obtain a dynamical system on an $(n-2)$ -dimensional ellipsoid $Q = \{E(\varpi) = \text{const}\} \subset \mathfrak{d}$.

Assume $\mathcal{J} \neq 0$. Then system (4.12) has a line of equilibria

$$\{\omega_{1n} = I_{1n} \tau, \dots, \omega_{n-1,n} = I_{n-1,n} \tau \mid \tau \in \mathbb{R}\}. \quad (4.14)$$

This line intersects the ellipsoid Q at two points, S^+ and S^- , which correspond to the stable and unstable steady-state rotations of the body in certain two-dimensional planes, fixed in both space and body. As shown in [7], all non-equilibrium solutions of system (4.12) lying on the same ellipsoid form heteroclinic connections from S^- to S^+ , *i.e.*, they approach S^- as $t \rightarrow -\infty$ and S^+ as $t \rightarrow \infty$. The motion of the n -dimensional body in space is an asymptotic evolution from a steady-state rotation in a two-dimensional plane fixed in the body, with angular velocity $-\omega$, to a steady-state rotation in the same plane, with angular velocity ω . The *spatial orientations* of the two-planes corresponding to the above steady-state rotations are typically *not* the same.

In the special case when $\mathcal{J} = 0$, *i.e.*, when the linear space $\mathfrak{d} \subset so(n)$ is an eigenspace for the inertia operator \mathbb{I} , all of the solutions of systems (4.11) and (4.12) are equilibria. Thus every motion of the body in space is a steady-state rotation. The reconstructed motion of the Suslov top on the group $SO(n)$ was studied in [27].

5 The Chaplygin Sleigh

The mechanical system reviewed in this section was introduced and studied in 1911 by Chaplygin [5] (the work had actually been finished in 1906). See [5] and [2] for a detailed exposition.

The Configuration Space. The sleigh is a rigid body moving on a horizontal plane supported at three points, two of which slide freely without friction while the third is a knife edge which allows no motion orthogonal to its direction. The configuration space of this dynamical system is $SE(2)$, the group of Euclidean motions of the two-dimensional plane \mathbb{R}^2 , which we parameterize with coordinates θ , the angular orientation of the blade, and (x, y) , the position of the contact point of the blade on the plane.

The Lagrangian and Constraint in the Body Frame. Introduce a coordinate system called the *body frame* by placing the origin at the contact point and choosing the first coordinate axis in the direction of the knife edge and the second coordinate axis in the orthogonal direction. Denote the angular velocity of the body by $\omega = \dot{\theta}$, and the components of the linear velocity of the contact point relative to the body frame by v_1 and v_2 . The vector (ω, v_1, v_2) is regarded as an element of the Lie algebra $se(2)$.

The Lagrangian equals the kinetic energy of the body, which is the sum of the kinetic energy of the center of mass and the rotational kinetic energy of the body. The position of the center of mass is specified by the coordinates (a, b) relative to the body frame. We do not assume here that $b = 0$ as in some models. We will see that a is crucial to the qualitative behavior of the system while b is irrelevant. Let m and J denote the mass and moment of inertia of the sleigh relative to the contact point, respectively.

The system is invariant with respect to the action of $SE(2)$ on $TSE(2)$ induced by the left action of $SE(2)$ on itself. The reduced Lagrangian is

$$l = \frac{1}{2} [(J + m(a^2 + b^2))\omega^2 + m(v_1^2 + v_2^2) - 2mb\omega v_1 + 2ma\omega v_2]. \quad (5.1)$$

The blade constraint reads

$$v_2 = -\dot{x} \sin \theta + \dot{y} \cos \theta = 0. \quad (5.2)$$

The Dynamics of the Chaplygin Sleigh. For the constrained motion, the angular momentum relative to the vertical axis through the contact point, M , and the components of the linear momentum relative to the moving frame, (Π_1, Π_2) , are computed to be

$$M = \frac{\partial l}{\partial \omega} = (J + m(a^2 + b^2))\omega - 2mbv_1, \quad \Pi_1 = \frac{\partial l}{\partial v_1} = m(v_1 - b\omega), \quad \Pi_2 = \frac{\partial l}{\partial v_2} = ma\omega.$$

The reduced dynamics of the Chaplygin sleigh is governed by the momentum equations (see [2])

$$\dot{M} = -\frac{a}{(J + ma^2)^2} (M + b\Pi_1) (mbM + (J + m(a^2 + b^2))\Pi_1), \quad \dot{\Pi}_1 = \frac{ma}{(J + ma^2)^2} (M + b\Pi_1)^2, \quad (5.3)$$

which are obtained from (2.6) by eliminating the Lagrange multiplier. In the particular case $b = 0$ they become

$$\dot{M} = -\frac{aM\Pi_1}{J + ma^2}, \quad \dot{\Pi}_1 = \frac{maM^2}{(J + ma^2)^2}. \quad (5.4)$$

Equations (5.3) preserve the reduced constrained energy

$$\frac{mM^2 + 2mbM\Pi_1 + (J + m(a^2 + b^2))\Pi_1^2}{2m(J + ma^2)}, \quad (5.5)$$

which is a positive-definite quadratic form.

We emphasize that the phase portrait of (5.3) is identical to that of the Suslov problem. Indeed, if $a = 0$, the nonholonomic momentum (M, Π_1) is conserved. Therefore, the body angular velocity ω and the linear velocity along the blade v_1 are constants. The evolution of the configuration variables (θ, x, y) is determined from the reconstruction equation (2.7), which reads

$$\dot{\theta} = \omega, \quad \dot{x} \cos \theta + \dot{y} \sin \theta = v_1, \quad -\dot{x} \sin \theta + \dot{y} \cos \theta = 0. \quad (5.6)$$

The solutions of (5.6) are

$$\theta = \theta_0 + \omega t, \quad x = x_0 + \frac{v_1}{\omega} \sin(\theta_0 + \omega t), \quad y = y_0 - \frac{v_1}{\omega} \cos(\theta_0 + \omega t) \quad \text{if } \omega \neq 0$$

and

$$\theta = \theta_0, \quad x = x_0 + tv_1 \cos \theta_0, \quad y = y_0 + tv_1 \sin \theta_0 \quad \text{if } \omega = 0.$$

Therefore, the contact point of the blade and the plane generically moves along a circle at a uniform rate.

If $a \neq 0$, the dynamics of (5.3) is integrable as the reduced energy is conserved. The trajectories are either equilibria situated on the line $M + b\Pi_1 = 0$, or elliptic arcs, as shown in Figure 5.1, left. Assuming $a > 0$, the equilibria located in the upper half plane are asymptotically stable (filled dots in Figure 5.1, left) whereas the equilibria in the lower half plane are unstable (empty dots). The elliptic arcs form heteroclinic connections between the pairs of equilibria.

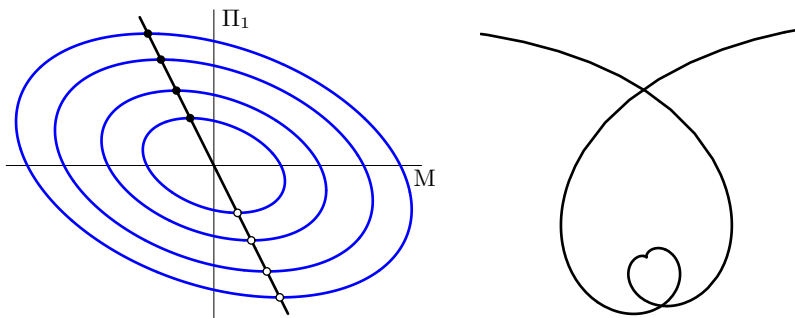


Figure 5.1: The momentum dynamics and the contact point trajectory for the Chaplygin sleigh.

As the momentum evolves along an elliptic arc, the contact point traces an interesting trajectory shown in Figure 5.1, right. This trajectory has a cusp as the speed of the contact point, $|v_1|$, momentarily vanishes when the momentum trajectory intersects the line $mbM + (J + m(a^2 + b^2))\Pi_1 = 0$, and asymptotically approaches uniform straight line motions as $t \rightarrow \pm\infty$.

The shape of the generic trajectory of the contact point is predetermined by the inertia of the body and the position of the center of mass relative to the blade, and is independent of the initial conditions. In particular, if $b = 0$, the trajectory of the contact point becomes axially-symmetric as shown in Figure 7.3. While the dynamics of the group variables (θ, x, y) cannot be explicitly written, it is possible to compute the angle between the asymptotic directions of the dynamics of the contact point. See [5] and [20] for details.

The Multidimensional Chaplygin Sleigh. We now briefly discuss the generalized Chaplygin sleigh, which is an n -dimensional rigid body moving in \mathbb{R}^n in the presence of certain nonholonomic constraints.

The configuration space of this dynamical system is the group $SE(n)$, which has the structure of a semidirect product, $SE(n) = SO(n) \ltimes \mathbb{R}^n$. The elements of $SE(n)$ are written as (g, x) , where $g \in SO(n)$ is the orthogonal rotation matrix that represents the orientation of the body

and $x \in \mathbb{R}^n$ is the position of a reference point of the body.⁵ It is often convenient to write the elements of $SE(n)$ as $(n+1) \times (n+1)$ matrices of the form

$$\begin{pmatrix} g & x \\ 0 & 1 \end{pmatrix}. \quad (5.7)$$

The group operations in $SE(n)$ are represented by products and inversions of matrices (5.7).

The Lie algebra $se(n)$ of the group $SE(n)$ has the structure of a semidirect product $so(n) \ltimes \mathbb{R}^n$. The elements of $se(n)$ are written (ξ, v) , where $\xi \in so(n)$ and $v \in \mathbb{R}^n$. The algebra $se(n)$ is isomorphic to the set of $(n+1) \times (n+1)$ matrices

$$\begin{pmatrix} \xi & v \\ 0 & 0 \end{pmatrix}, \quad \xi \in so(n), \quad v \in \mathbb{R}^n,$$

and the Lie bracket operation in $se(n)$ is given by the formula

$$[(\xi_1, v_1), (\xi_2, v_2)] = ([\xi_1, \xi_2], \xi_1 v_2 - \xi_2 v_1).$$

For a trajectory $(g(t), x(t)) \subset SE(n)$, the quantities $\omega = g^{-1}\dot{g}$ and $v = g^{-1}\dot{x}$ are the angular velocity of the body and the linear velocity of the reference point relative to the body frame, respectively. Let $a \in \mathbb{R}^n$ be the coordinates, relative to the body frame, of the center of mass of the body, which in general is located off the reference point. Denote the mass of the body and inertia operator with respect to the center of mass by m and \mathbb{I} , respectively (recall that $\mathbb{I}\omega = J\omega + \omega J$). Then the reduced Lagrangian is

$$\begin{aligned} l(\omega, v) &= -\frac{1}{4}\text{Tr}(\eta \mathbb{J} \eta^T) = \frac{1}{2} [(\mathbb{I}\omega, \omega) + m\|\omega a + v\|^2] \\ &= -\frac{1}{4}\text{Tr}(\omega(J + ma \otimes a)\omega) + m\langle a\omega, v \rangle + \frac{m}{2}\langle v, v \rangle, \end{aligned} \quad (5.8)$$

where

$$\eta = \begin{pmatrix} \omega & v \\ 0 & 0 \end{pmatrix} \in se(n), \quad \mathbb{J} = S \begin{pmatrix} J & 0 \\ 0 & m \end{pmatrix} S^T, \quad \text{and} \quad S = \begin{pmatrix} e & a \\ 0 & 1 \end{pmatrix} \in SE(n).$$

The body momentum $p = (M, \Pi)$ is an element of the dual Lie algebra $se^*(n)$ whose components are

$$M = \frac{\partial l}{\partial \omega} \in so^*(n), \quad \Pi = \frac{\partial l}{\partial v} \in \mathbb{R}^n, \quad (5.9)$$

that is, M and Π are the body angular and linear momenta, respectively. Straightforward evaluation of (5.9) leads to the formulae

$$M = (J + ma \otimes a)\omega + \omega(J + ma \otimes a) + m(v \otimes a - a \otimes v), \quad \Pi = m(v + \omega a). \quad (5.10)$$

Left-Invariant Constraints on $SE(n)$. There are numerous ways to introduce non-holonomic constraints for the generalized Chaplygin sleigh. For example, one can require that the velocity of the reference point is restricted to a subspace fixed in the body. For $n = 3$, systems with such constraints were studied in [20] and [28].

Another natural choice is to define the constraint subspace $\mathfrak{d} \in se(n)$ to be the set of matrices of the form

$$\begin{pmatrix} 0 & -\omega_{12} & \dots & -\omega_{1n} & v_1 \\ \omega_{12} & 0 & \dots & 0 & 0 \\ \vdots & \vdots & \ddots & \vdots & \vdots \\ \omega_{1n} & 0 & \dots & 0 & 0 \\ 0 & 0 & \dots & 0 & 0 \end{pmatrix}, \quad (5.11)$$

⁵The velocity of the reference point is typically constrained, like in the classical Chaplygin sleigh. For this reason the reference point is also called the contact point.

i.e., to impose Chaplygin-like constraints on the linear velocity and Suslov-like constraints on the angular velocity of the body. In particular, for $n = 2$ we obtain the classical Chaplygin constraint $v_2 = 0$, and (5.11) becomes

$$\begin{pmatrix} 0 & -\omega & v_1 \\ \omega & 0 & 0 \\ 0 & 0 & 0 \end{pmatrix}. \quad (5.12)$$

6 The Discrete Suslov Problem

Here we utilize the discrete Euler–Poincaré–Suslov equations (3.10) to construct the discretization of the Suslov problem considered in Section 4.

The Discrete Lagrangian. Let $g_k \in SO(n)$ be the orthogonal matrix that represents the position of the n -dimensional body.

Introduce the *incremental finite rotation* $\Omega_k = g_k^{-1}g_{k+1}$, which should be interpreted as the discrete analogue of the body angular velocity $\omega = g^{-1}\dot{g}$, as discussed in Section 3. If $g_k = g$ and $g_{k+1} = g_k + h\dot{g} + O(h^2)$, then

$$\lim_{h \rightarrow 0} \frac{\Omega_k - e}{h} = \lim_{h \rightarrow 0} \frac{g_k^{-1}g_{k+1} - e}{h} = g^{-1}\dot{g} = \omega. \quad (6.1)$$

Using the general approach, we compute the discrete Lagrangian and the reduced discrete Lagrangian for the Suslov problem to be

$$L_d(g_k, g_{k+1}) = \frac{1}{2} \text{Tr}(g_k J g_{k+1}^T), \quad l_d(\Omega_k) = \frac{1}{2} \text{Tr}(\Omega_k J), \quad (6.2)$$

where J represents the mass tensor.⁶ According to definition (3.2), the discrete body angular momentum of the top is

$$M_k = \Omega_k J - J \Omega_k^T \in \mathfrak{so}(n). \quad (6.3)$$

Using (6.1), one obtains $\lim_{h \rightarrow 0} M_k/h = \omega J + J \omega = M$, *i.e.*, the angular momentum of the continuous-time Suslov problem.

The Discrete Constraints. Following the approach of Section 2, we impose the discrete left-invariant constraints on $SO(n) \times SO(n)$ in the form of restrictions on the finite rotations $\Omega_k \in SO(n)$. In agreement with the continuous constraints (4.9), we assume that constrained rotations are the exponentials of the elements of the linear subspace

$$\mathfrak{d} = \text{span}\{e_1 \wedge e_n, \dots, e_{n-1} \wedge e_n\} \subset \mathfrak{so}(n).$$

The properties of the incremental finite rotations for the discrete Suslov problem are stated in the following lemma.

Lemma 6.1. *Let $\mathcal{S} = \exp \mathfrak{d}$ and $\Omega \in \mathcal{S}$. Then:*

- (i) *The components of the constrained finite rotation matrices Ω relative to the basis e_1, \dots, e_n satisfy the conditions*

$$\Omega_{ij} = \Omega_{ji}, \quad \Omega_{in} = -\Omega_{ni}, \quad 1 \leq i, j \leq n-1. \quad (6.4)$$

- (ii) *The subvariety \mathcal{S} is diffeomorphic to the projective space $\mathbb{RP}^{n-1} = S^{n-1}/\mathbb{Z}^2$. Given a point $(z_0, z_1, \dots, z_{n-1})$ on the unit sphere S^{n-1} , the components Ω_{ij} are*

$$\Omega_{ij} = \delta_{ij} - 2z_i z_j, \quad \Omega_{in} = -\Omega_{ni} = 2z_0 z_i, \quad \Omega_{nn} = 2z_0^2 - 1, \quad 1 \leq i, j \leq n-1. \quad (6.5)$$

⁶Definitions (6.2) and (6.3) were originally introduced in [19].

Note that the limit procedure (6.1) transforms formulae (6.4) into the Suslov constraints (4.10) on $so(n)$.

Proof. (i) Any vector from the subspace $\mathfrak{d} \subset so(n)$ can be represented as $\theta u \wedge e_n$, where θ is a scalar constant and $u = (u_1, \dots, u_{n-1}, 0)$ is a unit vector in $\text{span}(e_1, \dots, e_{n-1})$. The odd powers of matrices $e_i \wedge e_n$ are skew-symmetric and have an $(n-1) \times (n-1)$ zero block in the upper left corner, whereas the even powers are symmetric, with zero elements in the last row and last column. Hence, the exponential of any linear combination of $e_i \wedge e_n$ satisfies (6.4).

(ii) The operator $\exp(\theta u \wedge e_n) \in SO(n)$ represents the rotation by the angle θ in the two-dimensional plane spanned by u and e_n . Therefore,

$$\begin{aligned} \exp(\theta u \wedge e_n) u &= u \cos \theta - e_n \sin \theta, \\ \exp(\theta u \wedge e_n) e_j &= e_j - u \langle e_j, u \rangle + (u \cos \theta - e_n \sin \theta) \langle e_j, u \rangle, \quad 1 \leq j \leq n-1, \\ \exp(\theta u \wedge e_n) e_n &= e_n \cos \theta + u \sin \theta. \end{aligned}$$

The right-hand sides of the above formulae are the columns of the matrix $\exp(\theta u \wedge e_n)$. Then, identifying $\exp(\theta u \wedge e_n)$ with Ω and setting

$$\cos \theta/2 = z_0, \quad u_i \sin \theta/2 = z_i, \quad 1 \leq i, j \leq n-1, \quad (6.6)$$

we arrive at expressions (6.5).

Formulae (6.6) and the trigonometric identities

$$\sin \theta/2 = \sin(\pi - \theta/2), \quad \cos \theta/2 = -\cos(\pi - \theta/2)$$

imply that the opposite points z and $-z$ on the unit sphere S^{n-1} correspond to the same constrained rotation $\exp(\theta u \wedge e_n)$. Therefore $\mathcal{S} = \exp \mathfrak{d}$ is diffeomorphic to $\mathbb{R}\mathbb{P}^{n-1}$. \square

Remark. Conditions (6.4) are equivalent to the discrete left-invariant constraints

$$\text{Tr}(g_k^{-1} e_j \wedge e_n g_{k+1} - g_{k+1}^{-1} e_j \wedge e_n g_k) = 0, \quad j = 1, \dots, n-1,$$

on $SO(n) \times SO(n)$.

The Discrete Constraints for the Classical Suslov Problem. Conditions (6.4) and formulae (6.5) in the three-dimensional case state that Ω is a finite rotation about an axis parallel to the vector

$$(z_2, -z_1, 0) \in \text{span}(e_1, e_2) \subset \mathbb{R}^3.$$

Indeed, the group $SO(3)$ is covered twice by the unit sphere $S^3 = \{q_0^2 + q_1^2 + q_2^2 + q_3^2 = 1\}$, where (q_0, q_1, q_2, q_3) are the *Euler–Rodriguez parameters*. Any matrix $W \in SO(3)$ can be written as

$$W = \begin{pmatrix} q_0^2 + q_1^2 - q_2^2 - q_3^2 & 2(q_1 q_2 + q_3 q_0) & -2(q_1 q_3 - q_2 q_0) \\ 2(q_1 q_2 - q_3 q_0) & q_0^2 + q_2^2 - q_1^2 - q_3^2 & -2(q_2 q_3 + q_0 q_1) \\ -2(q_1 q_3 + q_2 q_0) & -2(q_2 q_3 - q_0 q_1) & q_0^2 + q_3^2 - q_1^2 - q_2^2 \end{pmatrix}; \quad (6.7)$$

see [26] for details. If $q_0 = \cos \theta/2$, the matrix W represents a rotation in \mathbb{R}^3 about the vector $e = (q_1, q_2, q_3)$ by the angle θ .

Setting $\Omega_{12} = \Omega_{21}$ in (6.7) implies $q_3 = 0$, and hence W is a rotation about an axis in the plane $\text{span}(e_1, e_2)$. Therefore, the constrained rotations $\Omega \in \mathcal{S} \subset SO(3)$ become

$$\Omega = \begin{pmatrix} 2(q_0^2 + q_1^2) - 1 & 2q_1 q_2 & 2q_0 q_2 \\ 2q_1 q_2 & 2(q_0^2 + q_2^2) - 1 & -2q_0 q_1 \\ -2q_0 q_2 & 2q_0 q_1 & 2q_0^2 - 1 \end{pmatrix}. \quad (6.8)$$

After the substitution $q_1 = -z_2$, $q_2 = z_1$, $q_0 = z_0$, formula (6.8) becomes identical to parameterization (6.5). As a result, the set of constrained rotations in the three-dimensional space is diffeomorphic to the real projective plane $\mathbb{R}\mathbb{P}^2 = S^2/\mathbb{Z}^2$. We emphasize that, in general, the k th position of the body, $g_k = \Omega_{k-1} \cdots \Omega_0$, is *not* a rotation in the plane $\text{span}(e_1, e_2)$.

Discrete Momentum Locus $\mathcal{U} \subset \mathfrak{so}^*(\mathbf{3})$. In contrast to the continuous case, the discrete momentum M_k does not evolve in a linear subspace in the dual Lie algebra $\mathfrak{so}^*(\mathbf{3})$. Instead, it belongs to the nonlinear algebraic variety $\mathcal{U} \subset \mathfrak{so}^*(\mathbf{3})$ defined by equations (6.3) and (6.8).

If the tensor J is diagonal in the frame e_1, e_2, e_3 ; $J = \text{diag}(J_1, J_2, J_3)$, then the vector representation $\mathbf{M} = \varphi(\mathbb{I}\Omega) = (M_{32}, M_{13}, M_{21})$ of the angular momentum reads

$$\mathbf{M} = 2((J_2 + J_3)q_0q_1, (J_1 + J_3)q_0q_2, (J_1 - J_2)q_1q_2),$$

where the discrete time index k has been omitted in order to avoid tedious notation. Here and below, without loss of generality, we always assume $q_0 \geq 0$. As a result, \mathcal{U} coincides with *the Steiner Roman surface* in \mathbb{R}^3 given by the quartic equation

$$\begin{aligned} \frac{J_1 - J_2}{(J_2 + J_3)(J_1 + J_3)} M_1^2 M_2^2 + \frac{J_1 + J_3}{(J_2 + J_3)(J_1 - J_2)} M_1^2 M_3^2 \\ + \frac{J_2 + J_3}{(J_1 + J_3)(J_1 - J_2)} M_2^2 M_3^2 - 2M_1 M_2 M_3 = 0 \end{aligned} \quad (6.9)$$

(see, e.g., [9] and [21]).

In the general case, when J is not diagonal, one recovers the parameterization

$$\mathbf{M} = 2 \begin{pmatrix} (J_{22} + J_{33})q_0q_1 - J_{12}q_0q_2 - (J_{13}q_1 + J_{23}q_2)q_2 \\ (J_{11} + J_{33})q_0q_2 - J_{12}q_0q_1 + (J_{13}q_1 + J_{23}q_2)q_1 \\ (J_{11} - J_{22})q_1q_2 - J_{12}(q_1^2 - q_2^2) - (J_{13}q_1 + J_{23}q_2)q_0 \end{pmatrix}. \quad (6.10)$$

One can show that the components of \mathbf{M} satisfy an algebraic equation of the fourth degree, which generalizes (6.9) and is not shown here. The corresponding algebraic surface \mathcal{U} in $\mathbb{R}^3 = \{(M_1, M_2, M_3)\}$ has pinch points and self-intersections. One can show that if the quadratic form $(J_{22} + J_{33})q_1^2 - 2J_{12}q_1q_2 + (J_{33} + J_{11})q_2^2$ is positive-definite, any point (M_1, M_2) has at most two real inverse images in \mathcal{U} . An example of the surface \mathcal{U} and its circular section for an unbalanced inertia tensor is given in Figure 6.1.

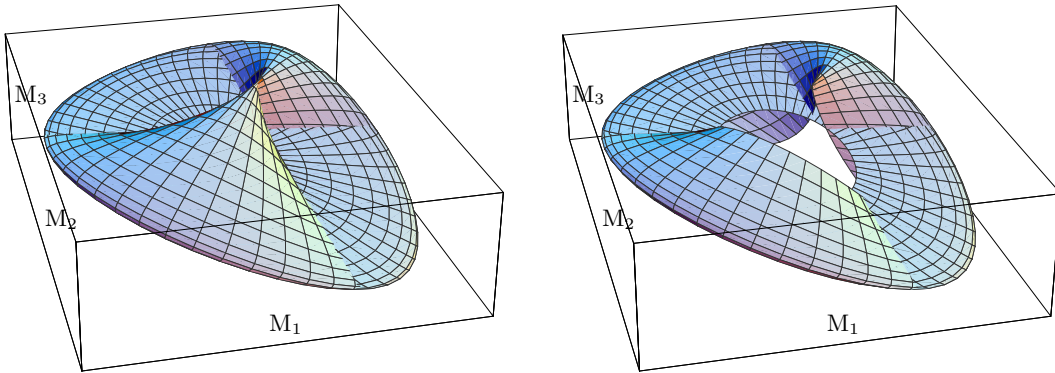


Figure 6.1: The momentum surface \mathcal{U} .

Discrete Euler–Poincaré–Suslov Equations on $\mathfrak{so}^*(\mathbf{3})$. In the case $G = SO(3)$, the discrete momentum equation with multipliers (3.10) becomes

$$M_{k+1} = \Omega_k^T M_k \Omega_k + \lambda_k \begin{pmatrix} 0 & 1 & 0 \\ -1 & 0 & 0 \\ 0 & 0 & 0 \end{pmatrix}, \quad (6.11)$$

where $M_k = \Omega_k J - J \Omega_k^T$ and the components of Ω_k are subject to the discrete constraint $\Omega_{12,k} = \Omega_{21,k}$. Equations (6.11) represent the dynamics of the discrete Suslov problem and define the maps $\mathcal{B} : \mathbb{RP}^2 \rightarrow \mathbb{RP}^2$ and $\mathcal{B}^* : \mathcal{U} \rightarrow \mathcal{U}$, which are generally multi-valued. For $(q_1 : q_2 : q_0) \in \mathbb{RP}^2$ we write $\mathcal{B}(q_1 : q_2 : q_0) = (\tilde{q}_1 : \tilde{q}_2 : \tilde{q}_0)$.⁷

To study map (6.11), we note that

$$\begin{aligned} \varphi(\Omega_k^T M_k \Omega_k) &= \varphi(J \Omega_k - \Omega_k^T J) = \Omega_k^T \mathbf{M}_k \\ &= 2 \begin{pmatrix} (J_{22} + J_{33})q_0 q_1 - J_{12}q_0 q_2 + (J_{13}q_1 + J_{23}q_2)q_2 \\ (J_{11} + J_{33})q_0 q_2 - J_{12}q_0 q_1 - (J_{13}q_1 + J_{23}q_2)q_1 \\ -(J_{11} - J_{22})q_1 q_2 + J_{12}(q_1^2 - q_2^2) - (J_{13}q_1 + J_{23}q_2)q_0 \end{pmatrix}, \end{aligned} \quad (6.12)$$

where \mathbf{M}_k denotes the vector representation of the discrete momentum.⁸ Using (6.10), we rewrite (6.11) in the vector form

$$\mathbf{M}_{k+1} = \mathbf{M}_k + 4 \begin{pmatrix} (J_{13}q_1 + J_{23}q_2)q_2 \\ -(J_{13}q_1 + J_{23}q_2)q_1 \\ -(J_{11} - J_{22})q_1 q_2 + J_{12}(q_1^2 - q_2^2) + \lambda_k \end{pmatrix}, \quad (6.13)$$

which is a discrete analogue of equations (4.3). This also shows that the momentum increment $\mathbf{M}_{k+1} - \mathbf{M}_k$ is orthogonal to the axis of rotation directed along the vector $(q_1, q_2, 0) \in \mathbb{R}^3$.

The map $\mathcal{B} : \mathbb{RP}^2 \rightarrow \mathbb{RP}^2$ given by (6.11) is evaluated as follows:

1. Given the input (q_1, q_2, q_0) , $q_0 = \sqrt{1 - q_1^2 - q_2^2} \geq 0$, one uses (6.10) and (6.12) to find the components of \mathbf{M}_k and of $\varphi(\Omega_k^T M_k \Omega_k)$, respectively.
2. Using the first two components of \mathbf{M}_{k+1} , one evaluates \tilde{q}_1 and \tilde{q}_2 by solving the system of two algebraic equations

$$\begin{aligned} M_{1,k+1} &= ((J_{22} + J_{33})\tilde{q}_1 - J_{12}\tilde{q}_2) \sqrt{1 - \tilde{q}_1^2 - \tilde{q}_2^2} - (J_{13}\tilde{q}_1 + J_{23}\tilde{q}_2)\tilde{q}_2, \\ M_{2,k+1} &= ((J_{11} + J_{33})\tilde{q}_2 - J_{12}\tilde{q}_1) \sqrt{1 - \tilde{q}_1^2 - \tilde{q}_2^2} + (J_{13}\tilde{q}_1 + J_{23}\tilde{q}_2)\tilde{q}_1, \end{aligned} \quad (6.14)$$

which are derived from (6.10). These equations define two quadratic surfaces Q_1 and Q_2 in $\mathbb{R}^3 = \{(q_1, q_2, q_0)\}$ that are symmetric about the origin of \mathbb{R}^3 . These surfaces intersect the unit sphere $\{q_1^2 + q_2^2 + q_0^2 = 1\}$ along certain curves C_1 and C_2 , respectively. Each curve is a union of two ovals, which are symmetric about the origin of \mathbb{R}^3 . One can show that the intersection of the curves C_1 and C_2 consists of four complex points and two or no real points in \mathbb{CP}^2 . Thus, there are at most two distinct real solutions $(\tilde{q}_1^{(j)}, \tilde{q}_2^{(j)}, \tilde{q}_0^{(j)})$ with $\tilde{q}_0^{(j)} > 0$.

3. One chooses a solution $(\tilde{q}_1^{(1)}, \tilde{q}_2^{(1)}, \tilde{q}_0^{(1)})$, with positive $\tilde{q}_0^{(1)}$, and then finds the last component of \mathbf{M}_{k+1} by the formula

$$M_{3,k+1} = (J_{11} - J_{22})\tilde{q}_1 \tilde{q}_2 - J_{12}(\tilde{q}_1^2 - \tilde{q}_2^2) - (J_{13}\tilde{q}_1 + J_{23}\tilde{q}_2)\tilde{q}_0,$$

which is obtained from (6.14) by replacing k with $k + 1$ and q with \tilde{q} .

In summary, the map $M_k \mapsto M_{k+1}$ given by (6.11) has in general four complex and two real values. In order to select one of these two real branches, we either use some extra arguments, like existence of a conservation law, or restrict ourselves to the case of sufficiently small q_1 and q_2 , which correspond to the small rotations Ω . In the latter case only one of the real solutions $(\tilde{q}_1^{(j)}, \tilde{q}_2^{(j)})$ is small, and it is natural to choose this small solution.

We now prove that the *constrained* energy (4.6) of the *continuous* Suslov system is preserved by the *discrete system* as well.

⁷The homogeneous coordinates on \mathbb{RP}^n are written as $(q_1 : \dots : q_n : q_0)$ in this paper.

⁸ Here and below, to simplify notation, we omit the discrete time index k in the components of q .

Theorem 6.2. *The discrete Suslov system (6.11) preserves the reduced constrained energy⁹*

$$E_c(\mathbf{M}_1, \mathbf{M}_2) = (J_{11} + J_{33})\mathbf{M}_1^2 + 2J_{12}\mathbf{M}_1\mathbf{M}_2 + (J_{22} + J_{33})\mathbf{M}_2^2. \quad (6.15)$$

Written as a function of (q_0, q_1, q_2) , (6.15) becomes the quartic conserved quantity

$$H = ((J_{22} + J_{33})q_1^2 - 2J_{12}q_1q_2 + (J_{11} + J_{33})q_2^2) \\ ((J_{13}q_1 + J_{23}q_2)^2 + [(J_{11} + J_{33})(J_{22} + J_{33}) - J_{12}^2]q_0^2). \quad (6.16)$$

The proof is straightforward: Substituting (6.10) into (6.15) and (6.12) into (6.15) produce identical outcomes.

The independence of the conservation law (6.15) from \mathbf{M}_3 is quite natural because all of the branches of the map (6.11) belong to the same level of the reduced constrained energy. We emphasize that the (unconstrained) energy $\frac{1}{2}\langle \mathbf{M}, \mathbb{I}^{-1}\mathbf{M} \rangle$ of the continuous Suslov problem is not preserved in the discrete setting.

The Invariant Curves on \mathbb{RP}^2 . As follows from Theorem 6.2, the map \mathcal{B} has invariant curves, which are either the intersections of the sphere $\{q_1^2 + q_2^2 + q_0^2 = 1\}$ with quartic surfaces $H(q) = c$ or, in the momentum space $so^*(3)$, intersections of the generalized quartic Steiner surface \mathcal{U} and the elliptic cylinders defined by (6.15). Thus, the invariant varieties are algebraic curves of order eight.

Assume that the kinetic energy metric is positive-definite, then the quadratic form $(J_{22} + J_{33})q_1^2 - 2J_{12}q_1q_2 + (J_{33} + J_{11})q_2^2$ is also positive-definite and, as follows from (6.16), the real invariant curves on the upper hemisphere $0 \leq q_0 \leq 1$ are unions of two branches. For small positive values of c one branch is a small oval around the origin $(0, 0)$, whereas the other branch is an oval close to the equator $\{q_0 = 0\}$ of the sphere. It may or may not intersect the equator. In the former case the opposite points of intersection are identified. The above branches correspond to the two connected components of the intersection of the Steiner surface \mathcal{U} and the cylinder.

As the energy value increases, the branches approach each other: The smaller one grows and the bigger one shrinks. At a certain critical value $c = c^*$ the branches touch at the two “saddle points” and form two separatrices. At the next critical value $c^{**} > c^*$ the two branches shrink to the two “center points”. There are no real invariant curves for $c > c^{**}$. Note that if $c = c^*$ or $c = c^{**}$, the elliptic cylinder (6.15) is tangent to the surface \mathcal{U} . The foliation of \mathbb{RP}^2 by invariant curves is illustrated in Figure 6.2.

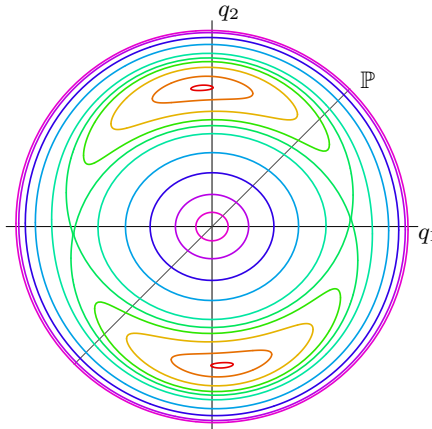


Figure 6.2: Invariant curves and the equilibrium line on \mathbb{RP}^2 .

⁹To simplify the exposition, we omit the denominator in (4.6).

Remark. As pointed out in [19], in the absence of nonholonomic constraints, the map $M_k \mapsto M_{k+1}$ given by the discrete Euler–Poincaré equations (6.11) is multi-valued because generically the equation $M_k = \Omega_k J - J \Omega_k^T$ has multiple solutions. In the presence of the discrete constraint $\Omega_{12,k} = \Omega_{21,k}$ the equation $M_k = \Omega_k J - J \Omega_k^T$ generally has a unique solution (excluding the self-intersection points of \mathcal{U}). However, as we saw above, the choice of λ_{k+1} or $M_{3,k+1}$ is not unique, and the map governing the dynamics of the discrete Suslov problem is multi-valued as well.

The Relative Equilibria of the Discrete Suslov Problem. According to (6.13), if the initial values q_1 and q_2 satisfy the condition $J_{13}q_1 + J_{23}q_2 = 0$, then

$$M_{1,k+1} = M_{1,k}, \quad M_{2,k+1} = M_{2,k}, \quad \varphi(\Omega_k^T M_k \Omega_k)_3 = -M_{3,k};$$

that is, the coadjoint action $M_k \mapsto \Omega_k^T M_k \Omega_k$ is the reflection with respect to the plane $\{M_3 = 0\}$. Therefore it is natural to assign to the multiplier λ_k the value that makes $M_{3,k+1}$ equal to $M_{3,k}$. Consequently, one of the branches of the map \mathcal{B} has a one-parameter family of equilibria. These equilibria are the points of the line

$$\mathbb{P} = (S^2 \cap \{J_{13}q_1 + J_{23}q_2 = 0\}) / \mathbb{Z}^2.$$

They represent the discrete analogues of the steady-state rotations of the body in the classical Suslov problem. According to (6.8), the points (q_1, q_2, q_0) and $(-q_1, -q_2, q_0)$ on \mathbb{P} correspond to the finite rotations Ω and Ω^T , respectively. It follows from (6.13) that there are no equilibrium points outside the line \mathbb{P} . In particular, neither the saddle points nor the centers of the invariant foliation of $\mathbb{R}\mathbb{P}^2$ are equilibria.

Finally, as in the continuous case, the only trajectories of the discrete Suslov problem with a balanced inertia tensor $J_{13} = J_{23} = 0$ are the equilibria, *i.e.*, the discrete body momentum M_k is preserved.

Remark. The geometry of the foliation of $\mathbb{R}\mathbb{P}^2$ by invariant curves suggests a natural way of selecting a branch of the map \mathcal{B} in the general case. Namely, if an initial point (q_1, q_2) lies in the open region $\mathcal{N} \subset \mathbb{R}\mathbb{P}^2$ distinguished by the condition $0 < c < c^*$, *i.e.*, (q_1, q_2) represents either a relatively small, or a sufficiently large finite rotation Ω , then the points (q_1, q_2) and $(\tilde{q}_1, \tilde{q}_2)$ belong to the same connected component of the invariant curve. In other words, for initial points from \mathcal{N} one should select a real solution of (6.14) that has either the smallest or the largest norm $\tilde{q}_1^2 + \tilde{q}_2^2$. On the other hand, a real initial point (q_1, q_2) that is located between the separatrices (that is, $(q_1, q_2) \in \mathbb{R}\mathbb{P}^2 \setminus \overline{\mathcal{N}}$) necessarily produces a complex output $(\tilde{q}_1, \tilde{q}_2)$. In particular, when the initial point is at a center, the next point is necessarily complex, although the value of the conservation law remains real.

If the branches of the map $\mathcal{B} : \mathbb{R}\mathbb{P}^2 \rightarrow \mathbb{R}\mathbb{P}^2$ are chosen as just discussed, the discrete-time dynamics in the region \mathcal{N} inherits all of the main properties of the continuous Suslov problem. Namely, let Δ_- , Δ_+ , Θ_- , and Θ_+ be the subsets of $\mathbb{R}\mathbb{P}^2$ defined by

$$\begin{aligned} \Delta_- &= \{J_{13}q_1 + J_{23}q_2 < 0\}, \\ \Delta_+ &= \{J_{13}q_1 + J_{23}q_2 > 0\}, \\ \Theta_- &= \{(J_{12}J_{13} + J_{22}J_{23} + J_{23}J_{33})q_1 - (J_{11}J_{13} + J_{12}J_{23} + J_{13}J_{33})q_2 < 0\}, \\ \Theta_+ &= \{(J_{12}J_{13} + J_{22}J_{23} + J_{23}J_{33})q_1 - (J_{11}J_{13} + J_{12}J_{23} + J_{13}J_{33})q_2 > 0\}. \end{aligned}$$

Theorem 6.3. *If the initial point $\mathbf{q} = (q_1, q_2)$ lies in $\mathcal{N} \subset \mathbb{R}\mathbb{P}^2$, then the sequence $\{\mathbf{q}_k\}$ belongs to the invariant curve through \mathbf{q} . As $k \rightarrow -\infty$, the sequence $\{\mathbf{q}_k\}$ approaches an unstable equilibrium on the half-line $\mathbb{P}_u = \mathbb{P} \cap \Theta_-$. As $k \rightarrow \infty$, the sequence $\{\mathbf{q}_k\}$ approaches a stable equilibrium on $\mathbb{P}_s = \mathbb{P} \cap \Theta_+$. Each sequence $\{\mathbf{q}_k\}$ lies entirely in either Δ_- or Δ_+ .*

Proof. First, we describe the discrete dynamics in the subset \mathcal{U}_0 of the momentum surface \mathcal{U} bounded by the condition

$$(J_{11} + J_{33})M_1^2 + 2J_{12}M_1M_2 + (J_{22} + J_{33})M_2^2 < c^*.$$

For this purpose introduce new coordinates on the M_1M_2 -plane:

$$\begin{aligned}\mu_1 &= (J_{13}(J_{11} + J_{33}) + J_{12}J_{23})M_1 + (J_{23}(J_{22} + J_{33}) + J_{12}J_{13})M_2, \\ \mu_2 &= J_{23}M_1 - J_{13}M_2.\end{aligned}$$

Using parameterization (6.10), we rewrite μ_1 and μ_2 as

$$\mu_1 = (J_{13}q_1 + J_{23}q_2) [Q + ((J_{11} + J_{33})(J_{22} + J_{33}) - J_{12}^2)q_0], \quad (6.17)$$

$$\mu_2 = Qq_0 - (J_{13}q_1 + J_{23}q_2)^2, \quad (6.18)$$

where

$$Q = (J_{12}J_{13} + J_{22}J_{23} + J_{23}J_{33})q_1 - (J_{11}J_{13} + J_{12}J_{23} + J_{13}J_{33})q_2.$$

The inequalities $(J_{11} + J_{33})(J_{22} + J_{33}) - J_{12}^2 > 0$ and $q_0 \geq 0$ imply that the quantity in the square brackets in (6.17) is positive throughout the region \mathcal{U}_0 . Hence the segment of the straight line $\mu_1 = 0$ inside \mathcal{U}_0 is filled out with equilibria of the map \mathcal{B} as the quantity $J_{13}q_1 + J_{23}q_2$ vanishes on this segment. Points in \mathcal{U}_0 with positive (negative) values of μ_1 correspond to the points in $\mathcal{N} \subset \mathbb{RP}^2$ with positive (negative) values of $J_{13}q_1 + J_{23}q_2$.

Next, (6.13) implies

$$\mu_{2,k+1} = \mu_{2,k} + 4(J_{13}q_{1,k} + J_{23}q_{2,k})^2,$$

and therefore the coordinate μ_2 always increases while the sequence $\{(\mu_{1,k}, \mu_{2,k})\}$ approaches the line $\mu_1 = 0$ along the ellipse $E_c(M_1, M_2) = \text{const}$. Then, as follows from (6.18), $\mu_2 < 0$, $Q < 0$ for $k \rightarrow -\infty$, and $\mu_2 > 0$, $Q > 0$ for $k \rightarrow \infty$. As a consequence, the unstable and stable equilibria fill out the sets $\mathbb{P}_u = \mathbb{P} \cap \Theta_-$ and $\mathbb{P}_s = \mathbb{P} \cap \Theta_+$, respectively.

From (6.13), $\mu_{1,k+1} - \mu_{1,k} = -(J_{13}q_{1,k} + J_{23}q_{2,k})Q$, and therefore

$$\mu_{1,k+1} = (J_{13}q_{1,k} + J_{23}q_{2,k})((J_{11} + J_{33})(J_{22} + J_{33}) - J_{12}^2)q_{0,k}.$$

This formula and (6.17) imply that $\mu_{1,k}$ and $\mu_{1,k+1}$ are always of the same sign unless $J_{13}q_1 + J_{23}q_2 = 0$, *i.e.*, the sequence $\{(\mu_{1,k}, \mu_{2,k})\}$ lies entirely in either $\mathcal{U}_0 \cap \{\mu_1 < 0\}$ or $\mathcal{U}_0 \cap \{\mu_1 > 0\}$.

Reformulating these properties for the dynamics in the region $\mathcal{N} \subset \mathbb{RP}^2$, we arrive at the statement of the theorem. \square

For the foliation in Figure 6.2, the corresponding discrete-time dynamics in the neighborhood of the origin of the M_1M_2 -plane is shown in Figure 6.3, where stable and unstable equilibria are the filled and empty dots, respectively. As follows from Theorem 6.3,

$$\lim_{k \rightarrow \infty} \Omega_k = \left(\lim_{k \rightarrow -\infty} \Omega_k \right)^{-1} = \text{const},$$

i.e., the discrete trajectories in the group $SO(3)$ approach the discrete steady-state rotations as $k \rightarrow \pm\infty$, which agrees perfectly with the asymptotic behavior of the continuous-time Suslov problem.

The Discrete Euler–Poincaré–Suslov Equations on $so^*(n)$. We now briefly discuss the case $G = SO(n)$, which retains all of the main features of the continuous n -dimensional Suslov problem.

The discrete momentum equation (3.10) is

$$M_{k+1} = \Omega_k^T M_k \Omega_k + \sum_{1 \leq i < j < n} \lambda_{ij} e^i \wedge e^j, \quad M_k = \Omega_k J - J \Omega_k^T, \quad (6.19)$$

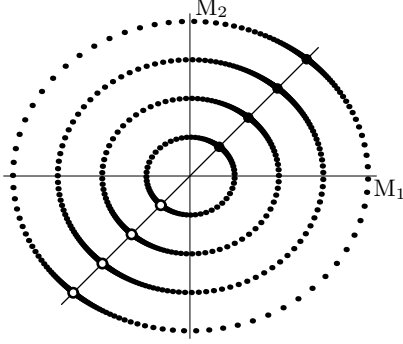


Figure 6.3: Discrete dynamics near the origin of $\mathbb{R}\mathbb{P}^2$.

where, as above, e_1, \dots, e_n is an orthonormal body frame, and the components of Ω_k are parameterized by the coordinates $(z_0 : z_1 : \dots : z_{n-1})$ on $\mathbb{R}\mathbb{P}^{n-1}$ as in (6.5). In this case the momentum M belongs to an $(n-1)$ -dimensional algebraic surface \mathcal{U} in $so^*(n) = \mathbb{R}^{n(n-1)/2}$.

Let π be the projection $so^*(n) \rightarrow \mathbb{R}^{n-1} = \{(M_{1n}, \dots, M_{n-1,n})\}$. The inverse image of a generic point in $\pi(\mathcal{U}) \subset \mathbb{R}^{n-1}$ is a union of a finite number of points in \mathcal{U} . Hence, one needs to choose one of many possible values of the multipliers λ_{ij} . Thus, (6.19) should be regarded as a multi-valued map $\mathcal{B} : \mathbb{R}^{n-1} \rightarrow \mathbb{R}^{n-1}$.

Recall that $\Lambda : \mathfrak{d} \rightarrow \mathfrak{d}^*$ is the restriction of the inertia operator $\mathbb{I} : so(n) \mapsto so^*(n)$ onto the subspace \mathfrak{d} . It is nondegenerate and in the above basis in \mathfrak{d} is given by the $(n-1) \times (n-1)$ matrix

$$\Lambda_{ij} = J_{ij} + J_{nn}\delta_{ij}, \quad i, j = 1, \dots, n-1.$$

To simplify the exposition, introduce the vectors

$$\mathcal{J} = (J_{1n}, \dots, J_{n-1,n}), \quad \mathcal{M} = (M_{1n}, \dots, M_{n-1,n}), \quad \mathcal{Z} = (z_1, \dots, z_{n-1}).$$

Then, using (6.3) and (6.5), we obtain

$$\mathcal{M}_k = 2z_{0,k}\Lambda\mathcal{Z}_k - 2(\mathcal{Z}_k \wedge \mathcal{J})\mathcal{Z}_k. \quad (6.20)$$

Next, equations (6.19) yield

$$\mathcal{M}_{k+1} = 2z_{0,k}\Lambda\mathcal{Z}_k + 2(\mathcal{Z}_k \wedge \mathcal{J})\mathcal{Z}_k = \mathcal{M}_k + 4(\mathcal{Z}_k \wedge \mathcal{J})\mathcal{Z}_k. \quad (6.21)$$

As seen from (6.21), the discrete Euler–Poincaré–Suslov equations on $so^*(n)$ have a line ℓ of equilibria, which is the image of the projective line $\mathbb{P} \subset \mathbb{R}\mathbb{P}^{n-1}$ defined by the equation $\mathcal{Z} \wedge \mathcal{J} = 0$, or, in coordinates,

$$(z_1 : z_2 : \dots : z_{n-1}) = (J_{1n} : J_{2n} : \dots : J_{n-1,n}).$$

Since for small \mathcal{Z} its components approximate the angular velocities $\omega_{1n}, \dots, \omega_{n-1,n}$ of the continuous multidimensional system (4.12), the line \mathbb{P} approximates line (4.14) of equilibrium points in $so(n)$.

Theorem 6.4. *The generalized Euler–Poincaré–Suslov dynamics has the following properties:*

- (i) *The multi-valued map \mathcal{B} preserves the reduced constrained energy*

$$\frac{1}{2}\langle \mathcal{M}, \Lambda^{-1}\mathcal{M} \rangle, \quad (6.22)$$

which, after using (6.20) and multiplying by $2 \det \Lambda$, yields the quartic conservation law

$$H = \langle \mathcal{Z}, \Lambda\mathcal{Z} \rangle (\langle \mathcal{Z}, \mathcal{J} \rangle^2 + z_0^2 \det \Lambda). \quad (6.23)$$

(ii) Regardless of which branch of the map \mathcal{B} is chosen, the discrete dynamics evolves from unstable equilibria on $\ell \cap \{\langle \mathcal{J}, \mathcal{M} \rangle < 0\}$ toward stable equilibria on $\ell \cap \{\langle \mathcal{J}, \mathcal{M} \rangle > 0\}$.

Proof. (i) Substituting formulae (6.20) and (6.21) into (6.22) produces identical results in terms of z -variables. Transforming this expression into the form (6.23) is a pure calculation.

(ii) Using (6.21), we obtain

$$\langle \mathcal{J}, \mathcal{M}_{k+1} \rangle = \langle \mathcal{J}, \mathcal{M}_k \rangle + 4 \sum_{1 < i < j < n} (\mathcal{Z}_k \wedge \mathcal{J})_{ij}^2.$$

Hence, the quantity $\langle \mathcal{J}, \mathcal{M} \rangle$ increases unless M belongs to the equilibrium set ℓ . \square

7 The Discrete Chaplygin Sleigh

In this section we study the discrete Euler–Poincaré–Suslov equation (3.10) on the dual Lie algebra $se^*(2)$. See [8] for an elementary exposition of this problem.

The Discrete Lagrangian. Recall that the angular orientation and position of the contact point of the sleigh are θ and (x, y) , respectively. The two subsequent positions of the sleigh are given by the matrices

$$g_k = \begin{pmatrix} \cos \theta_k & -\sin \theta_k & x_k \\ \sin \theta_k & \cos \theta_k & y_k \\ 0 & 0 & 1 \end{pmatrix}, \quad g_{k+1} = \begin{pmatrix} \cos \theta_{k+1} & -\sin \theta_{k+1} & x_{k+1} \\ \sin \theta_{k+1} & \cos \theta_{k+1} & y_{k+1} \\ 0 & 0 & 1 \end{pmatrix}.$$

The incremental displacement $W_k = g_k^{-1}g_{k+1} \in SE(2)$ is computed to be

$$W_k = \begin{pmatrix} \cos \Delta\theta_k & -\sin \Delta\theta_k & \cos \theta_k \Delta x_k + \sin \theta_k \Delta y_k \\ \sin \Delta\theta_k & \cos \Delta\theta_k & -\sin \theta_k \Delta x_k + \cos \theta_k \Delta y_k \\ 0 & 0 & 1 \end{pmatrix}, \quad (7.1)$$

where $\Delta\theta_k = \theta_{k+1} - \theta_k$, $\Delta x_k = x_{k+1} - x_k$, and $\Delta y_k = y_{k+1} - y_k$.

Following the general formula (3.1), we compute the left-invariant discrete Lagrangian on $SE(2) \times SE(2)$ by replacing the velocity operator with $g_k^{-1}(g_{k+1} - g_k)$ in (5.8). Up to an additive constant, we obtain

$$L_d(g_{k+1}, g_k) = \frac{1}{2} \text{Tr}(W_k \mathbb{J} W_k^T) - \frac{1}{2} \text{Tr}(\mathbb{J} W_k^T + W_k \mathbb{J}), \quad (7.2)$$

where

$$\mathbb{J} = \begin{pmatrix} J/2 + ma^2 & mab & ma \\ mab & J/2 + mb^2 & mb \\ ma & mb & m \end{pmatrix}.$$

Recall that J is the moment of inertia of the body relative to its center of mass, m is the mass, and (a, b) are the coordinates of the center of mass of the body measured from the contact point in the directions along and orthogonal to the blade. Evaluating (7.2), we obtain

$$\begin{aligned} L_d = & (J + ma^2 + mb^2)(1 - \cos \Delta\theta_k) + \frac{m}{2} \Delta y_k^2 + \frac{m}{2} \Delta x_k^2 \\ & + am[(\cos \theta_{k+1} - \cos \theta_k) \Delta x_k + (\sin \theta_{k+1} - \sin \theta_k) \Delta y_k] \\ & + bm[-(\sin \theta_{k+1} - \sin \theta_k) \Delta x_k + (\cos \theta_{k+1} - \cos \theta_k) \Delta y_k]. \end{aligned} \quad (7.3)$$

Observe that setting

$$\begin{aligned} \Delta\theta_k &= h\omega + O(h^2), & \Delta x_k &= h\dot{x} + O(h^2), & \Delta y_k &= h\dot{y} + O(h^2), \\ \cos \theta_{k+1} - \cos \theta_k &= -h\omega \sin \theta + O(h^2), & \sin \theta_{k+1} - \sin \theta_k &= h\omega \cos \theta + O(h^2), \end{aligned} \quad (7.4)$$

and computing the limit

$$\lim_{h \rightarrow 0} l_d/h^2$$

produces the continuous-time Lagrangian of the Chaplygin sleigh (5.1).

According to definition (3.2), the components of the discrete momentum relative to the body frame, $p_k = (M_k, \Pi_{1,k}, \Pi_{2,k}) \in se^*(2)$, are

$$\begin{aligned} M_k &= -\frac{\partial}{\partial s} \Big|_{s=0} L_d(\theta_k + s, \theta_{k+1}, x_k, x_{k+1}, y_k, y_{k+1}) \\ \Pi_{1,k} &= -\frac{\partial}{\partial s} \Big|_{s=0} L_d(\theta_k, \theta_{k+1}, x_k + s \cos \theta_k, x_{k+1}, y_k + s \sin \theta_k, y_{k+1}), \\ \Pi_{2,k} &= -\frac{\partial}{\partial s} \Big|_{s=0} L_d(\theta_k, \theta_{k+1}, x_k - s \sin \theta_k, x_{k+1}, y_k + s \cos \theta_k, y_{k+1}), \end{aligned}$$

that is,

$$\begin{aligned} M_k &= (J + ma^2 + mb^2) \sin \Delta\theta_k + amV_{2,k} - bmV_{1,k}, \\ \Pi_{1,k} &= mV_{1,k} - am(1 - \cos \Delta\theta_k) - bm \sin \Delta\theta_k, \\ \Pi_{2,k} &= mV_{2,k} + am \sin \Delta\theta_k - bm(1 - \cos \Delta\theta_k), \end{aligned} \tag{7.5}$$

where

$$V_{1,k} = \Delta x_k \cos \theta_k + \Delta y_k \sin \theta_k, \quad V_{2,k} = -\Delta x_k \sin \theta_k + \Delta y_k \cos \theta_k \tag{7.6}$$

are the components of the ‘‘discrete velocity’’ of the center of mass relative to the body frame.

In the absence of constraints the dynamics of the two-dimensional body is represented by the discrete Euler–Poincaré equations

$$p_{k+1} = \text{Ad}_{W_k}^* p_k, \tag{7.7}$$

where

$$\text{Ad}_{W_k}^* p_k = \begin{pmatrix} M_k - \Pi_{2,k}V_{1,k} + \Pi_{1,k}V_{2,k} \\ \Pi_{1,k} \cos \Delta\theta_k + \Pi_{2,k} \sin \Delta\theta_k \\ -\Pi_{1,k} \sin \Delta\theta_k + \Pi_{2,k} \cos \Delta\theta_k \end{pmatrix}. \tag{7.8}$$

Equation (7.7) is just the momentum conservation law written in the body frame. In particular, if the center of mass is at the contact point, that is $a = b = 0$, (7.7) becomes

$$\begin{aligned} \sin \Delta\theta_k &= \sin \Delta\theta_{k-1}, \\ \Delta x_{k+1} \cos \theta_{k+1} + \Delta y_{k+1} \sin \theta_{k+1} &= \Delta x_k \cos \theta_{k+1} + \Delta y_k \sin \theta_{k+1}, \\ -\Delta x_{k+1} \sin \theta_{k+1} + \Delta y_{k+1} \cos \theta_{k+1} &= -\Delta x_k \sin \theta_{k+1} + \Delta y_k \cos \theta_{k+1}. \end{aligned}$$

If $\Delta\theta$ is sufficiently small, the above formulae imply that the increments $\theta_{k+1} - \theta_k$, $x_{k+1} - x_k$, and $y_{k+1} - y_k$ are the same for any integer k , the result one expects from studying the continuous problem.

The Discrete Constraint on $SE(2)$. We now impose a discrete left-invariant constraint on $SE(2) \times SE(2)$ in the form of restrictions on the incremental displacements $W_k = g_k^{-1}g_{k+1}$. A tempting choice of a discrete constraint that mimics the non-slip condition (5.2) is

$$V_{2,k} = -\sin \theta_k \Delta x_k + \cos \theta_k \Delta y_k = 0. \tag{7.9}$$

This choice however is not the right one. Indeed, following our general approach (3.4), constrained incremental displacements are the exponents of the matrices of the form (5.11). In this case \mathfrak{h} generates the subgroup $SE(n-1)$ and, according to Proposition 3.1, $\exp \mathfrak{d}$ covers the homogeneous space $SE(n)/SE(n-1)$. For a matrix $W \in SE(n)$, we write its components as W_{ij} . In the case $n = 2$, when W_k is given by (7.1), we have:

Theorem 7.1. *The variety $\mathcal{S} = \exp \mathfrak{d} \subset SE(2)$ is diffeomorphic to the canonical line bundle $\pi : \mathbb{M} \rightarrow \mathbb{RP}^1 = \{(z_1 : z_2)\}$ such that $\pi^{-1}(z_1 : z_2)$ is a line $\{(\tau z_1, \tau z_2) \mid \tau \in \mathbb{R}\} \subset \mathbb{R}^2$ (i.e., \mathbb{M} is an unbounded Möbius strip). Analytically, \mathcal{S} is represented by the equation*

$$\frac{W_{23}}{W_{13}} = \frac{1 - W_{11}}{W_{21}}, \quad (7.10)$$

which defines the discrete constraint

$$-(\Delta x_k \cos \theta_k + \Delta y_k \sin \theta_k) \sin \frac{\Delta \theta_k}{2} + (-\Delta x_k \sin \theta_k + \Delta y_k \cos \theta_k) \cos \frac{\Delta \theta_k}{2} = 0 \quad (7.11)$$

or, equivalently,

$$V_{1,k}(1 - \cos \Delta \theta_k) - V_{2,k} \sin \Delta \theta_k = 0. \quad (7.12)$$

Proof. For an element

$$\xi = \begin{pmatrix} 0 & -\omega & v \\ \omega & 0 & 0 \\ 0 & 0 & 0 \end{pmatrix} \in \mathfrak{d}$$

we have

$$W = \exp \xi = \begin{pmatrix} \cos \omega & -\sin \omega & \frac{v}{\omega} \sin \omega \\ \sin \omega & \cos \omega & \frac{v}{\omega} (1 - \cos \omega) \\ 0 & 0 & 1 \end{pmatrix},$$

where ω and v are arbitrary. As a result, (7.10) holds for $W_k \in \mathcal{S}$. Next, for $\omega = \Delta \theta_k$ we obtain

$$\frac{W_{23}}{W_{13}} = \frac{1 - \cos \omega}{\sin \omega} = \tan \frac{\Delta \theta_k}{2}, \quad (7.13)$$

which implies (7.11) and (7.12).

Finally, formula (7.13) represents the slope of the line $W_{23}x - W_{13}y = 0$ in the plane \mathbb{R}^2 . As $\Delta \theta_k$ increases from 0 to 2π , this line rotates by the angle π . Hence, \mathcal{S} is diffeomorphic to the Möbius strip. \square

Corollary 7.2. *The discrete left-invariant Chaplygin constraint on $SE(2) \times SE(2)$ reads*

$$\mathcal{F} = -\sin \left(\frac{\theta_{k+1} + \theta_k}{2} \right) \Delta x_k + \cos \left(\frac{\theta_{k+1} + \theta_k}{2} \right) \Delta y_k = 0. \quad (7.14)$$

The limit $\lim_{h \rightarrow 0} \mathcal{F}/h$, with $\Delta \theta_k$, Δx_k , and Δy_k defined as in (7.4), equals the continuous-time Chaplygin constraint (5.2).

Remark. As seen from (7.11), the matrices from $\mathcal{S} \subset SE(2)$ represent ‘‘circular displacements’’ of the sleigh: The points (x_k, y_k) and (x_{k+1}, y_{k+1}) in \mathbb{R}^2 belong to a circle, with the blade directions at these points tangent to the same circle. This property also implies

$$\begin{aligned} \Delta x_k \cos \theta_k + \Delta y_k \sin \theta_k &= \Delta x_k \cos \theta_{k+1} + \Delta y_k \sin \theta_{k+1}, \\ -\Delta x_k \sin \theta_k + \Delta y_k \cos \theta_k &= \Delta x_k \sin \theta_{k+1} - \Delta y_k \cos \theta_{k+1}, \end{aligned} \quad (7.15)$$

see Figure 7.1.

The discrete Chaplygin constraint (7.11) has also the following interpretation: In order to transfer the sleigh from $(\theta_k, x_k, y_k) \in SE(2)$ to $(\theta_{k+1}, x_{k+1}, y_{k+1}) \in SE(2)$ (assuming that this transition is possible), one needs first to perform the rotation by $\Delta \theta_k/2$ at (x_k, y_k) , which aims the sleigh towards (x_{k+1}, y_{k+1}) , then slide the sleigh from (x_k, y_k) to (x_{k+1}, y_{k+1}) , and then perform additional rotation by $\Delta \theta_k/2$ at (x_{k+1}, y_{k+1}) .

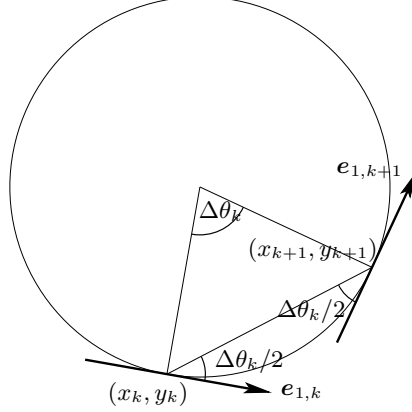


Figure 7.1: The geometry of the incremental displacements for the Chaplygin sleigh.

The Discrete Momentum Locus $\mathcal{U} \subset se^*(2)$. One can show that in the presence of constraint (7.12) the image of the discrete Legendre transform (7.5) is an algebraic quartic subvariety $\mathcal{U} \subset se^*(2) = \{(M, \Pi_1, \Pi_2)\}$ and that there are four inverse images of a generic point (M, Π_1) in $\mathcal{S} \subset SE(2)$. Here we concentrate on the important case $b = 0$, when the structure of the real surface $\mathcal{U} \subset se^*(2)$ becomes simpler.

Let \mathcal{L} be the discrete Legendre transform. Put $\mathcal{V} = \{p \in \mathcal{U} \mid \mathcal{L}^{-1}(\mathcal{V}) = SO(2) \subset SE(2)\}$. It is more convenient to study the images $\tilde{\mathcal{U}}$ and $\tilde{\mathcal{V}}$ of the surface \mathcal{U} and set \mathcal{V} in \mathbb{R}^3 parameterized by the coordinates (M, Y, Z) , where $Y = a\Pi_1 + 2ma^2$, $Z = \sin \Delta\theta$.

Lemma 7.3. *Let $b = 0$. Then:*

(i) *The surface $\tilde{\mathcal{U}}$ is given by the cubic polynomial equation*

$$J^2 Z^3 - 2JMZ^2 + (Y^2 + 2JY + M^2)Z - 2MY = 0 \quad (7.16)$$

and lies between and is tangent to the planes $Z = \pm 1$ along the lines $\ell_{\pm} = \{\pm M - Y = J\}$. The M and Y axes belong entirely to $\tilde{\mathcal{U}}$.

(ii) *For the parts of $\tilde{\mathcal{U}}$ over the quadrants*

$$\{-Y + M > J\} \cap \{-Y - M > J\} \quad \text{and} \quad \{-Y + M < J\} \cap \{-Y - M < J\}$$

the quantity $\cos \Delta\theta$ is positive, i.e., $-\pi/2 < \Delta\theta < \pi/2$, and in the rest of the quadrants $\cos \Delta\theta$ is negative, i.e., $\pi/2 < \Delta\theta < 3\pi/2$.

(iii) *The projection $\tilde{\pi} : \tilde{\mathcal{U}} \rightarrow \mathbb{R}^2 = \{(M, Y)\}$ is one-to-one everywhere but in the interior of the triangular region bounded by the discriminant curve*

$$Y^4 + 6JY^3 + Y^2(12J^2 + 2M^2) - Y(10JM^2 - 8J^3) + M^4 - J^2M^2 = 0$$

which is symmetric with respect to the Y -axis, is tangent to the M -axis at the origin $(0, 0)$, and has three cusp points. Within the region bounded by this curve the projection $\tilde{\pi}$ is three-to-one.

(iv) *The projection of the set $\tilde{\mathcal{V}} \subset \tilde{\mathcal{U}}$ onto the MY -plane is the ellipse*

$$\mathcal{E} = \{M = (J + ma^2) \sin \Delta\theta, Y = ma^2(1 + \cos \Delta\theta) \mid \Delta\theta \in (0, 2\pi)\}. \quad (7.17)$$

The points of $\tilde{\mathcal{U}}$ with $V_1 < 0$ ($V_1 > 0$) are projected inside (outside) the ellipse \mathcal{E} .

Note that the point $(M, Y) = (0, 2ma^2)$ corresponds to the origin in the $M\Pi_1$ -plane and that the projection $\tilde{\pi}$ is one-to-one in a neighborhood of this point. An example of the surface $\tilde{\mathcal{U}}$ and its projection onto the MY -plane for $J = 1.5$, $m = 0.3$, and $a = 1$ is presented in Figure 7.2. The shaded region in Figure 7.2, right, represents the set where the projection $\tilde{\pi}$ is three-to-one.

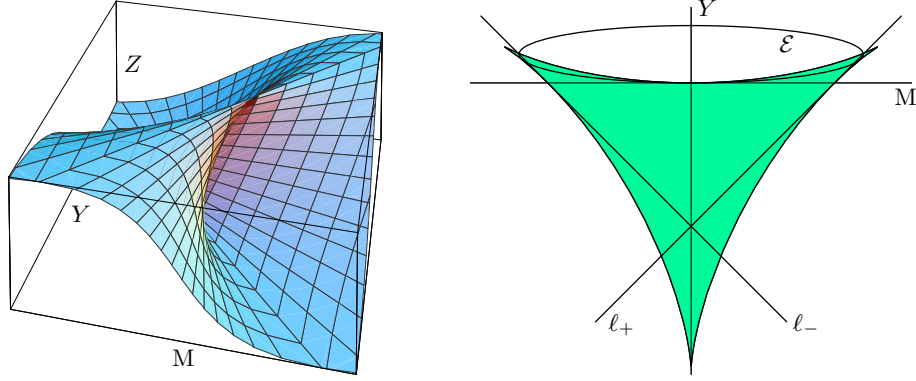


Figure 7.2: The surface $\tilde{\mathcal{U}}$ and its projection onto the MY -plane.

Proof. (i) Using condition (7.12), we eliminate Π_1 and Π_2 from the first two equations of system (7.5) and obtain the following equation for $\Delta\theta_k$:

$$J \sin^2 \Delta\theta_k - M_k \sin \Delta\theta_k + (2ma^2 + a\Pi_{1,k})(1 - \cos \Delta\theta_k) = 0. \quad (7.18)$$

This equation always has trivial solutions $\Delta\theta_k = 2n\pi$, $n \in \mathbb{Z}$. Setting $\sin \Delta\theta_k = Z$, $\cos \Delta\theta_k = \sqrt{1 - Z^2}$, and $Y = a\Pi_1 + 2ma^2$, we arrive at a quartic polynomial equation with respect to Z , which has the root $Z = 0$. Factoring out Z and omitting the index k , one obtains the cubic equation (7.16). By setting $z = \pm 1$ in (7.16) we obtain $(J \mp M + Y)^2 = 0$, which implies that $\tilde{\mathcal{U}}$ is indeed tangent to the planes $Z = \pm 1$ along the lines ℓ_{\pm} . Finally, setting $Z = M = 0$ or $Z = Y = 0$, one sees that equation (7.16) becomes an identity for an arbitrary Y and M , respectively.

(ii) For a fixed $(M, \tilde{\Pi}_1)$, each root of (7.16) gives a solution of (7.18), with the sign of $\cos \Delta\theta_k$ appropriately chosen. As seen from (7.18), for $|\Pi_1|$ large and $z = \sin \Delta\theta$ small the value of $\cos \Delta\theta$ is close to 1, whereas for M positive and large and $|\Pi_1|$ small the value of $\cos \Delta\theta$ is negative. The sign of $\cos \Delta\theta$ can change only when a point in the $M\Pi_1$ -plane moves from one quadrant to another. This finishes the proof of part (ii).

Parts (iii) and (iv) are verified by straightforward calculations. \square

The Discrete Constrained Dynamics on $se^*(2)$. According to (3.10), the discrete Euler–Poincaré–Suslov equations for the Chaplygin sleigh read

$$p_{k+1} = \text{Ad}_{W_k}^* p_k + \lambda_k(0, 0, 1), \quad (7.19)$$

with $\text{Ad}_{W_k}^* p_k$ given by formula (7.8). Eliminating the Lagrange multiplier λ_k from (7.19), we obtain

$$\begin{aligned} M_{k+1} &= (J + ma^2 + mb^2) \sin \Delta\theta_k - bmV_{1,k} + am[-\Delta x_k \sin \theta_{k+1} + \Delta y_k \cos \theta_{k+1}], \\ \Pi_{1,k+1} &= mV_{1,k} - bm \sin \Delta\theta_k + am[\Delta x_k \cos \theta_{k+1} + \Delta y_k \sin \theta_{k+1}], \end{aligned}$$

which, when (7.15) and (7.5) are taken into account, yield

$$M_{k+1} = M_k - 2amV_{2,k}, \quad \Pi_{1,k+1} = \Pi_{1,k} + 2am(1 - \cos \Delta\theta_k). \quad (7.20)$$

Formulae (7.20) and (7.12) define multi-valued maps $\mathcal{U} \rightarrow \mathcal{U}$ and $\mathcal{S} \rightarrow \mathcal{S}$. These maps are evaluated as follows:

1. Given $\Delta\theta_k$ and $V_{1,k}$, one finds $V_{2,k}$ from constraint (7.12) and then computes $(M_k, \Pi_{1,k}, \Pi_{2,k})$ as an output of the Legendre transform (7.5).

2. Next, one finds M_{k+1} and $\Pi_{1,k+1}$ from (7.20).
3. Finally, one finds $\Delta\theta_{k+1}$ and $V_{1,k+1}$ by solving the system of equations

$$\begin{aligned} M_{k+1} &= (J + ma^2 + mb^2) \sin \Delta\theta_{k+1} + \left(am \frac{1 - \cos \Delta\theta_{k+1}}{\sin \Delta\theta_{k+1}} - bm \right) V_{1,k+1}, \\ \Pi_{1,k+1} &= mV_{1,k+1} - am(1 - \cos \Delta\theta_{k+1}) - bm \sin \Delta\theta_{k+1} \end{aligned}$$

obtained from (7.5) and (7.12) by replacing k with $k + 1$.

Theorem 7.4. *Equations (7.20) preserve the reduced constrained energy of the continuous-time Chaplygin sleigh*

$$E_c(M, \Pi_1) = \frac{mM^2 + 2bmM\Pi_1 + (J + m(a^2 + b^2))\Pi_1^2}{m(J + ma^2)}. \quad (7.21)$$

Proof. Evaluating $E_c(M_{k+1}, \Pi_{1,k+1})$ and $E_c(M_k, \Pi_{1,k})$ while taking into account equations (7.5), (7.20), and constraint (7.12), one recovers identical expressions in terms of $\Delta\theta_k$, $V_{1,k}$ and $V_{2,k}$. \square

Since the quadratic form (7.21) is positive-definite, the invariant manifolds of map (7.20) are the ellipses in the $M\Pi_1$ -plane.

The Relative Equilibria of the Discrete Chaplygin Sleigh. As follows from (7.20), the initial conditions $\{\Delta\theta_k = 0, V_{2,k} = 0\}$ imply $M_{k+1} = M_k$, and $\Pi_{1,k+1} = \Pi_{1,k}$. Hence, it is natural to choose such λ_k in (7.19) that $\Pi_{2,k+1} = \Pi_{2,k}$ as well. Thus, similar to the continuous system (5.3), for $a \neq 0$ the map (7.19) has a family of equilibria. These equilibria are situated on the line $\{M + b\Pi_1 = 0\}$ in the $M\Pi_1$ -plane and correspond to the translations of the contact point in the xy -plane along the direction of the blade by constant increments.

On the other hand, for $a = 0$ every solution of (5.3) is an equilibrium. That is, contrary to the unconstrained case, the components of momentum relative to the body frame, rather than the spatial components, are preserved. Equations (7.5) in this case imply $\Delta\theta_{k+1} = \Delta\theta_k$, $V_{1,k+1} = V_{1,k}$. Therefore, the discrete trajectories of the contact point in the xy -plane are either straight lines or circles. In the latter case the radius equals $V_{1,k}/\sin(\Delta\theta_k)$. The same behavior occurs in the continuous-time, balanced ($a = 0$) sleigh.¹⁰

The Unbalanced Case. In this case $a \neq 0$, and we set $b = 0$ for simplicity. Then the map $(M_k, \Pi_{1,k}) \mapsto (M_{k+1}, \Pi_{1,k+1})$ has a line of equilibria $M = 0$ and, by Theorem 7.4, the nonequilibrium discrete trajectories lie on the invariant ellipses $mM^2 + (J + ma^2)\Pi_1^2 = \text{const}$. Without loss of generality, we assume $a > 0$. Then the following property holds:

Theorem 7.5. *The map $(M_k, \Pi_{1,k}) \mapsto (M_{k+1}, \Pi_{1,k+1})$ is single-valued in the elliptic neighborhood of the origin of the $M\Pi_1$ -plane given by the condition*

$$mM^2 + (J + ma^2)\Pi_1^2 < m^2a^2(J + ma^2). \quad (7.22)$$

The orbits of this map form heteroclinic connections between the pairs of unstable and stable equilibria similar to that of the continuous-time Chaplygin sleigh. That is, the sequence $\{(M_k, \Pi_{1,k})\}$ approaches a stable (unstable) equilibrium along the corresponding invariant ellipse as $k \rightarrow \infty$ ($k \rightarrow -\infty$). In both cases the sequence $\{(M_k, \Pi_{1,k})\}$ remains in one of the half-planes $M < 0$ or $M > 0$.

¹⁰Numerical simulations show that the choice of the ‘naive’ constraint (7.9) instead of (7.10) in the case $a = 0$ results in spiraling discrete trajectories in the xy -plane.

Proof. Part (iii) of Lemma 7.3 implies that the map is single-valued in the region (7.22). Next, as follows from the first formula in (7.20) for $a > 0$, the increment $\Pi_{1,k+1} - \Pi_{1,k}$ is always greater than or equal to zero. Thus, to prove the asymptotic behavior one only needs to show that the sequence $\{(M_k, \Pi_{1,k})\}$ lies entirely in one of the half-planes $M < 0$ or $M > 0$. Indeed, assume first that the point $(M_k, \Pi_{1,k})$ from the neighborhood (7.22) lies also inside the ellipse \mathcal{E} in (7.17) and that $M_k > 0$. Then equation (7.11) and parts (ii) and (iv) of Lemma 7.3 imply that $V_{1,k}$ and $V_{2,k}$ are negative. According to (7.20), the increment $M_{k+1} - M_k$ is then positive. Similarly, for $M_k < 0$ one has $M_{k+1} - M_k < 0$. Hence, in this case M_k and M_{k+1} have the same sign.

Next, using (7.5) and (7.11), if the point $(M_k, \Pi_{1,k})$ lies in the region (7.22) but outside the ellipse \mathcal{E} , then $2amV_{2,k} > M_k$ for $M_k > 0$ and $2amV_{2,k} < M_k$ for $M_k < 0$. Invoking (7.20), M_k and M_{k+1} again have the same sign, which completes the proof. \square

Observe that the discrete-time momentum dynamics of the Chaplygin sleigh in the neighborhood of the origin is similar to that of the Suslov problem, illustrated in Figure 6.3.

We conclude this section with an example of the discrete sleigh trajectory in the xy -plane. The dots in Figure 7.3 represent the generic discrete trajectory of the contact point in this plane while the continuous-time trajectory is the solid curve. The discrete dynamics captures

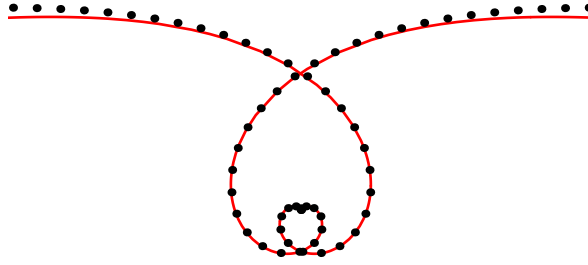


Figure 7.3: A typical discrete sleigh trajectory.

the qualitative behavior of the continuous-time Chaplygin sleigh. In particular, the discrete trajectory has a cusp and asymptotically approaches the straight line motions as $k \rightarrow \pm\infty$.

8 Conclusions

The discrete nonholonomic Suslov problem and the discrete Chaplygin sleigh that we introduced in this paper remarkably inherit all of the main properties of their corresponding continuous-time dynamical systems. In particular, they preserve the reduced constrained energy and, in the balanced case, the momentum. It is not currently clear if this behavior is due to the low dimension of the systems, or if it is possible to construct completely solvable discretizations of the Suslov and Chaplygin problems. These issues will be addressed in future publications.

Our approach can be adapted to study discretizations of nonholonomic LR systems on Lie groups. For such systems, the Lagrangian is left-invariant while the constraint distribution is *right*-invariant. The discrete dynamics of such systems, as well as the existence of their invariant measure, is currently being developed and will be exposed in a future publication.

Acknowledgments

YNF's research was partially supported by Spanish Ministry of Science and Technology grant BFM 2003-09504-C02-02; DVZ's research was partially supported by NSF grant DMS-0306017.

References

- [1] Arnold, V.I., V.V. Kozlov, and A.I. Neishtadt [1989], *Mathematical Aspects of Classical and Celestial Mechanics. Dynamical System III*, Springer-Verlag, New York.
- [2] Bloch, A. M. [2003], *Nonholonomic Mechanics and Control*. Interdisciplinary Applied Mathematics **24**, Springer-Verlag.
- [3] Bloch A. M., P. S. Krishnaprasad, J. E. Marsden, and R. Murray [1996], Nonholonomic Mechanical Systems with Symmetry. *Arch. Rational Mech. Anal.* **136**, 21–99.
- [4] Bobenko A. I. and Y. B. Suris [1999], Discrete Lagrangian Reduction, Discrete Euler–Poincaré Equations, and Semidirect Products. *Lett. Math. Phys.* **49**, 79–93.
- [5] Chaplygin, S. A. [1911], On the Theory of Motion of Nonholonomic Systems. The Theorem on the Reducing Multiplier. *Math. Sbornik XXVIII*, 303–314, (in Russian).
- [6] Cortés J. and Martínez S. [2001], Nonholonomic Integrators. *Nonlinearity* **14**, 1365–1392.
- [7] Fedorov Yu. N. and V. V. Kozlov [1995], Various Aspects of n -Dimensional Rigid Body Dynamics. *Amer. Math. Soc. Transl* **168**, 141–171.
- [8] Fedorov, Yu. N. and D. V. Zenkov [2004], Dynamics of the Discrete Chaplygin Sleigh. *Discrete and Continuous Dynamical Systems, to appear*.
- [9] Gray, A. [1997], *Modern Differential Geometry of Curves and Surfaces with Mathematica*, 2nd ed. Boca Raton, FL: CRC Press.
- [10] Jovanović, B. [2001], Geometry and Integrability of Euler–Poincaré–Suslov Equations. *Nonlinearity* **14**, 1555–1657.
- [11] Helgason, S. [1962], *Differential Geometry and Symmetric Spaces*. Academic Press, New York.
- [12] Kozlov, V. V. [1985], On the Integration Theory of Equations of Nonholonomic Mechanics. *Advances in Mechanics* **8**, 85–107 (in Russian).
- [13] Kozlov, V. V. [1988], Invariant Measures of the Euler–Poincaré Equations on Lie algebras. *Funct. Anal. Appl.* **22**, 58–59.
- [14] de León, M., D. Martín de Diego, and A. Santamaría Merino [2002], Geometric Integrators and Nonholonomic Mechanics. arXiv:math-ph/0211028.
- [15] McLachlan, R. [1993], Explicit Lie–Poisson Integration and the Euler Equations. *Phys. Rev. Lett.* **71**, 3043–3046.
- [16] Marsden, J. E., S. Pekarsky, and S. Shkoller [1999], Discrete Euler–Poincaré and Lie–Poisson Equations. *Nonlinearity* **12**, 1647–1662.
- [17] Marsden, J. E. and T. S. Ratiu [1999], *Introduction to Mechanics and Symmetry*. Texts in Applied Mathematics **17**, Springer-Verlag.
- [18] Marsden, J. E. and M. West [2001], Discrete mechanics and variational integrators. *Acta Numerica* **10**, 357–514.
- [19] Moser, J. and A. Veselov [1991], Discrete Versions of Some Classical Integrable Systems and Factorization of Matrix Polynomials. *Comm. Math. Phys.* **139**, 217–243.
- [20] Neimark, Ju. I. and N. A. Fufaev [1972], *Dynamics of Nonholonomic Systems*. Translations of Mathematical Monographs **33**, AMS, Providence.
- [21] Steiner’s Roman Surface. <http://mathworld.wolfram.com/romansurface.html>.
- [22] Suslov, G. [1902], *Theoretical Mechanics*, Vol. 2, Kiev (in Russian).
- [23] Veselov, A. P. [1988], Integrable Discrete-Time Systems and Difference Operators. *Funct. Anal. Appl.* **22**, 1–13.
- [24] Veselov, A. P. [1991], Integrable Lagrangian Correspondences and the Factorization of Matrix Polynomials. *Funct. Anal. Appl.* **25**, 38–49.

- [25] Wendland, J. M, and J. E. Marsden [1997], Mechanical Integrators Derived from a Discrete Variational Principle. *Physica D* **106**, 223–246.
- [26] Whittaker, E. T. [1960], *A Treatise on Analytical Dynamics*, 4th ed. Cambridge Univ. Press, Cambridge.
- [27] Zenkov, D. V. and A. M. Bloch [2000], Dynamics of the n -Dimensional Suslov problem. *J. Geom. Phys.* **34**, 121–136.
- [28] Zenkov, D. V. and A. M. Bloch [2003], Invariant Measures of Nonholonomic Flows with Internal Degrees of Freedom. *Nonlinearity* **16**, 1793–1807.
- [29] Zenkov, D. V. [2003], Linear Conservation Laws of Nonholonomic Systems with Symmetry. *Discrete and Continuous Dynamical Systems (extended volume)*, 963–972.